

Czech Technical University in Prague
Faculty of Mechanical Engineering

Department of Automotive, Combustion Engine and Railway Engineering
Master of automotive engineering
Advanced Powertrains



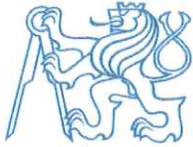
**Analysis of the DNOx 2.2 system's equalizing
membrane stress**

DIPLOMA THESIS

Author: Bc. Marek Pitra

Supervisor: Ing. Michal Vašíček, Ph.D.

Year: 2017



CZECH TECHNICAL UNIVERSITY IN PRAGUE

Faculty of Mechanical Engineering,

Department of Automotive, Combustion Engine and Railway Engineering

Technická 4, 166 07 Praha 6

School year: 2016/2017

DIPLOMA THESIS ASSIGNMENT

Student: **Bc. Marek PITRA**

Study program: **N2307 Master of Automotive Engineering**

Field of study: **2301T050 Advanced Powertrains**

Title: **Analysis of the DNOx 2.2 system's equalizing membrane stress**

Assignment:

The aim of the thesis is to determine and verify critically stressed areas of the part during the real operation (real or duty cycle) with use of an FEM and physical measurements.



Thesis extent: minimally 55 pages

Graphical extent:

Specialized literature list:

Supervisor: Ing. Michal Vašíček, Ph.D.

Specialist:

Date of thesis assignment: 24 October 2016

Deadline of submission: 6 January 2017

If the student does not submit his/her thesis in time he/she must justify in advance this fact in writing. If the dean recognizes this excuse (handed to the Dean via the Study Department) he will grant the student an alternative term for his/her State Final Exam (two terms still remain). If the student does not present a relevant excuse or if the dean does not recognize the excuse, he will also grant the student an alternative term for his/her State Final Exam. In this case, however, only one term of the State Final Exam remains (Student Examination Code, Art.22, par.3, 4.)

The student acknowledges that he/she must elaborate the project by himself/herself, without any help except consultations with his/her supervisor. A list of used literature, other sources and names of consultants must be listed in the thesis.

I received the assignment on (date): 10.11.2016

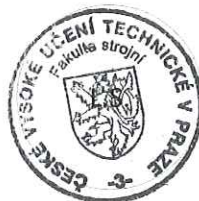
Student's signature

Doc. Ing. Oldřich VÍTEK, Ph.D.

Head of Department

Prof. Ing. Michael VALÁŠEK, DrSc.

Dean



Prague, 24 October 2016

Disclaimer

I hereby declare that this thesis is my own work and that, to the best of my knowledge and belief, it contains no material which has been accepted or submitted for the award of any other degree or diploma. I also declare that all the software used to solve this thesis is legal.

I also declare that, to the best of my knowledge and belief, this thesis contains no material previously published or written by any other person except where due reference is made in the text of the thesis.

.....

Date

.....

Bc. Marek Pitra

Acknowledgment

I would like to thank my supervisors from CTU and Robert Bosch company, namely Ing. Michal Vašíček, Ph.D. and Ing. Lukáš Franta Ph.D., for their kind guidance, advice and leading through this thesis. My thanks also belong to Ing. Hynek Chlup from Departement of Biomechanics who kindly help me with physical measurement of the membrane material. Last but not least, I would like to thank my parents for their support during whole period of my studies and also many thanks belongs to my girlfriend for her kindness and support.

Bc.Marek Pitra

Title: *Analysis of the DNOx 2.2 system's equalizing membrane stress*

Author: Bc. Marek Pitra

Study program: Master of Automotive Engineering

Field of study: Advanced Powertrains

Assignment: Diploma Thesis

Supervisor: Ing. Michal Vašíček, Ph.D.

Department of Automotive, Combustion Engine and Railway Engineering,

Faculty of Mechanical Engineering, Czech Technical University in Prague

Abstract: This thesis describes stress of equalizing membrane of DNO_x 2.2. supply module. Behaviour of membrane is simulated in ABAQUS FEA software. There are determined critically stressed areas and proposed design modifications in order to achieve stress reduction. Part of the thesis is dedicated to material model verification with use of real measurement.

Key words: ABAQUS, FEA, Denoxtronic, stress analysis, hyper elasticity

Content

Introduction.....	12
1 After treatment systems	13
1.1 In – cylinder control	14
1.2 After treatment systems.....	14
2 Selective catalytic reduction	15
2.1 Ammonia SCR	15
2.2 Mechanism of SCR system	17
2.3 SCR catalyst	19
3 Denoxtronic systems.....	20
3.1 Denoxtronic 2.2.....	20
3.2 Functional principle of Denoxtronic 2.2	20
3.3 Supply module	22
3.4 Diaphragm pump.....	24
3.5 Material of flutter membrane	25
4 Description of the problem	25
4.1 Start/Stop test	27
4.2 Phases of Start/Stop test	28
4.2.1 Pressure build-up phase	28
4.2.2 Dosing phase.....	29
4.2.3 Back Sucking phase	29
5 Identification and validation of material model.....	31
5.1 Preparation of the samples	31
5.2 Procedure of sample connection to the tool and testing rig	37
6 Physical measurement.....	42
6.1 Data post-processing	42

6.2	Result of measurement	45
7	FEA simulation of physical measurement	45
7.1	Simulation settings	45
7.2	Comparison of stress strain curves from simulation and measurement.....	51
8	FEA simulation of real and modified designs	51
8.1	Evaluation of real design results	58
8.2	Analysis of modified design results	61
8.3	Comparison of results	63
	Conclusion	66

List of figures

Figure 1: Diesel exhaust SCR technology	18
Figure 2: Comparison of different SCR catalyst technologies – NOx conversion [10].	19
Figure 3: Diagram of Denoxtronic 2.2 system [5].....	21
Figure 4: Detailed technical features of Denoxtronic 2.2 system [5]	22
Figure 5: Exploded model of Supply module	23
Figure 6: Flutter membrane - region description	24
Figure 7: Location of area with highest possibility of crack type failure	27
Figure 8: Start stop cycle [16].....	28
Figure 9: Pressure in oscillating chamber	29
Figure 10: Shapes of samples with approximate dimensions	32
Figure 11: Final shape of samples	33
Figure 12: Locations of cuts	33
Figure 13: Real sample measuring on microscope with software ruler.....	34
Figure 14: Set of samples prepared for testing	36
Figure 15: Model of aluminium tool with general dimensions	37
Figure 16: Prepared sample with paper attached	38
Figure 17: Sample assembled with tool - top view.....	38
Figure 18: Sample assembled with tool - side view	38
Figure 19: Sample assembled with tool - bottom view	39
Figure 20: Assembly prepared to be attached to the testing rig.....	39
Figure 21: Sample with marks attached to testing rig - ready for testing.....	40
Figure 22: Optical strain monitoring and measurement	41
Figure 23: Stress strain curves for all measured samples	44
Figure 24 ABAQUS simulation - Load settings.....	48
Figure 25: Meshed sample with C3D8RD elements	49

Figure 26: Comparison of material models with real measurement on short samples ...	50
Figure 27:: Comparison of material models with real measurement on long samples...	50
Figure 28: Steps of 2D model creation	52
Figure 29: Properties of Housing to Membrane interaction	55
Figure 30: Properties of Plate to Membrane interaction.....	55
Figure 31: Meshed 2D assembly	58
Figure 32: Membrane after compression - end of "Mounting" step	59
Figure 33: Membrane under overpressure load of 7 bar.....	59
Figure 34: Membrane under overpressure load of 9 bar.....	60
Figure 35: Stress in observed area under over pressusre loads.....	60
Figure 36: Design optimization 1 - end of 9bar over pressure step	62
Figure 37: Design optimization 2 - end of 9bar over pressure step	62
Figure 38: Design optimization 3 - end of 9bar over pressure step	63
Figure 39: Comparison of modified designs with real design in terms of stress observed in critical area.....	63

List of tables

Table 1: EU Emissions Standards for Passanger Cars [3]	13
Table 2: AdBlue physical and chemical properties [6].....	16
Table 3: Property of HNBR material [16]	25
Table 4: Samples dimensions and evaluation - first set.....	34
Table 5: Samples dimensions and evaluation - second set	35
Table 6: Properties of each step	54
Table 7: Mounting amplitude	56
Table 8: Amplitude of regular pressure	57
Table 9: Amplitude of 7 bar overpressure	57
Table 10: Amplitude of 9 bar overpressure	57
Table 11: Table of maximal and final stress values of real and modified designs.	64
Table 12: Improvement achieved by design modifications in terms of percentage improvement comparing to real design.	64

List of Abbreviations

FEA	Finite Element Analysis
EU	European Union
SCR	Selective Catalytic Reduction
SM	Supply Module
SI	Spark Ignition
CI	Combustion Ignition
EGR	Exhaust Gas Recirculation
US EPA	United States Environmental Protection Agency
DEF	Diesel Engine Fluid
ECU	Engine Control Unit
DCU	Dosing Control Unit
DPF	Diesel Particulate Filter
DOC	Diesel Oxidation Catalyst
DM	Dosing Module
HNBR	Hydrogenated Nitrile Butadiene Rubber
RBCB	Robert Bosch České Budějovice
CTU	Czech Technical University
CAE	Computer Aided Engineering
SW	Software
BC	Boundary Conditions
DOF	Degrees of Freedom
TWC	Three Way Catalyst

Introduction

Since the first mass-produced car, Ford Model T, was introduced to public, passenger cars aspired to be an integral part of our lives. Emissions of passenger cars was not important issue until the number of cars begin to increase rapidly. If we look on traffic density (number of cars per 1000 inhabitants) operating in European Union (EU) in segment of passenger cars, this value grows rapidly over the last few decades. During the period of time from 1993 to 2009 the traffic density of EU grew from 322 to 419 cars per 1000 inhabitants. On the top of that, average EU traffic density in 2014 was 487 cars per one thousand of inhabitants [12] [13]. If we also consider the fact that population of EU is constantly growing during this period of time, then it is obvious that total number of cars is greatly increasing and so it is necessary to control the emissions of vehicles [14]. European Union propose more and more strict and binding legislation for combustion engine emissions which car producers has to follow. Since the combustion engines are reaching almost their physical limits and tuning of engine cycle could not lower the emissions enough than after treatment of exhaust gas is inevitable.

This thesis is focused on stress analysis of one small subpart of Denoxtronic 2.2 selective catalytic reduction (SCR) system which is being produced by Robert Bosch company. This system in general reduces the emissions of NO_x gasses from compression ignition (CI) engines in order to fulfil European emission standards (EURO). In this thesis will be analysed stress of small rubber component called flutter membrane. Stress analysis is required due to the fact that during specific test of Supply module (SM) was observed that some SM failed due to damaged flutter membrane component. Because of this failure it was necessary to investigate the reason of membrane failure and ideally propose the solution how to avoid this damage. Reader of this thesis may realize, as same as I did, that even failure of at the first sight unimportant, small component with price of few Euro cents could cause malfunction of whole SCR after treatment system with value of thousands of Euros.

1 After treatment systems

With increasing density of traffic all over the world, there is a pressure on car producers to reduce harmful exhaust gasses due to the strict government regulations. As you can see in table 1, limits are stricter with each new incoming regulation. I would like also point out fact, that allowed amount of NO_x is lower with each new emission regulation, compare to level of CO, which remains same since 2005. [1]

Stage	Valide since	CO	HC	HC+NO _x	NO _x	PM	PN
		g/km					
Compression Ignition engines (Diesel)							
Euro 1	1992/07	2,72	-	0,97	-	0,14	-
Euro 2,IDI	1996/01	1.0	-	0,7	-	0,08	-
Euro 2,DI	1996/01 ^a	1.0	-	0,9	-	0,1	-
Euro 3	2000/01	0.64	-	0,56	0,5	0,05	-
Euro 4	2005/01	0.50	-	0,3	0,25	0,025	-
Euro 5a	2009/09 ^b	0.50	-	0,23	0,18	0,005	-
Euro 5b	2011/09 ^c	0.50	-	0,23	0,18	0,005	6,0×10 ¹¹
Euro 6	2014/09	0.50	-	0,17	0,08	0,005	6,0×10 ¹¹
Spark Ignition engines (Gasoline)							
Euro 1	1992/07	2,72	-	0,97	-	-	-
Euro 2	1996/01	2,2	-	0,5	-	-	-
Euro 3	2000/01	2,3	0,2	-	0,15	-	-
Euro 4	2005/01	1	0,1	-	0,08	-	-
Euro 5	2009/09 ^b	1	0,1	-	0,06	0,005 ^e	-
Euro 6	2014/09	1	0,1	-	0,06	0,005 ^e	6,0×10 ^{11 e}

a) until 1999.09.30 (after that date DI engines must meet the IDI limits)

b) 2011.01 for all models

c) 2013.01 for all models

e) applicable only to vehicles using DI engines

Table 1: EU Emissions Standards for Passenger Cars [3]

Due to strict emissions limits, there have been proposed and applied many approaches to control NO_x emissions, which could be divided into two categories:

- I. In – cylinder control
- II. After treatment systems

1.1 In – cylinder control

In – cylinder control reduces NO_x emissions before and during combustion phase by decreasing temperature of gas and by controlling chemical combustion reactions. Technologies for in – cylinder controls are listed below:

- Optimizing spark timing for SI engines and injection timing for CI engines.
- Using EGR (Exhaust Gas Recirculation) to control peak temperature in combustion chamber and chemical reactions
- Intercooling of boosted intake charge to control temperature

1.2 After treatment systems

After treatment systems allow us to reduce already formed NO_x. These systems are based on chemical reactions of exhaust gas with other chemical components and catalysts. Into this category belong these systems:

- Three-way catalyst (TWC) for Spark ignition (SI) engines
- Selective catalytic reduction (SCR) for Compression ignition (CI) engines

As it is mentioned, in SI engine is used three-way catalyst, which could not be used in CI engines. This restriction is based on fact that SI engines operate at or near to stoichiometric air/fuel ratio. This condition provides enough reducing gasses for sufficient NO_x reduction. On the other hand, CI engines operate with much higher air/fuel ratio with approximate range from $\lambda=1,2$ during full throttle to $\lambda=4$ in idle operation. Due to higher air/fuel ratio, using of TWC in CI engines is impossible. The result of this fact is a need of another system for NO_x reduction in CI engines called “Selective catalytic reduction” system. [1] [2] [11]

2 Selective catalytic reduction

SCR system is based on conversion of harmful oxides of nitrogen (NO_x) into harmless nitrogen (N₂) and water vapour (H₂O) via catalytic reaction. Engines operating with lean air/fuel mixture intake unavoidably more oxygen than could be used in combustion process. According to this fact, exhaust gas contains significant level of oxygen, which makes reduction of NO_x in oxygen-rich atmosphere chemically unlikely. Due to this fact, SCR system is needed in CI engines. [1] [2]

First application of SCR was in 1970s in thermal power plants in Japan. Later on, there was wide spread of SCR application in Europe and US. In mid-2000s, the first SCR system was adapted for mobile diesel engines by Nissan diesel in Japan and Daimler in Europe. As far as United States, there were SCR systems introduced by car producers mostly in 2010 for a purpose to meet US EPA NO_x limits for heavy duty trucks, which are one of the most stringent in the world. In order to achieve almost zero NO_x emissions, there are two technologies based on different reductant chemistry:

- Ammonia SCR
- Hydrocarbon SCR

2.1 Ammonia SCR

This system use ammonia as a reductant, which could be in three forms:

- I. Pure ammonia
- II. Aqueous ammonia
- III. Urea

Pure ammonia is toxic and hazardous and also require pressurized tanks due to high vapour pressure. According to this requirement, it is not suitable for mobile engine utilization, but could be used in large industrial stational SCR operators.

Aqueous ammonia is much safer to use and transport, but it must be hydrolysed in order to be used as reductant.

For purpose of this thesis only SCR technology using ammonia in form of urea solution will be described.

Urea is the safest form of ammonia storage. It meets requirements for easy and complete decomposition into ammonia, producing no harmful side-products under condition of SCR reactor. This solution is easy to storage and transport, inexpensive and commonly available.

Urea, $\text{CO}(\text{NH}_2)_2$, is used in form of Diesel Engine Fluid (DEF). This designation is used mainly in USA. In Europe is known under commercial name “AdBlue”.

AdBlue is 32,5% solution of synthetic high purity urea in distilled water. Physical and chemical properties of AdBlue are listed in following table 2.

Physical state:	Liquid
Colour:	Colourless, yellowish
Odor:	Ammoniacal (slightly)
pH:	10
Boiling/condensation point:	103°C
Freezing/melting point:	-11°C
Density:	1,087 to 1,093 g/cm ³ [20°C]
Dynamic viscosity:	0,14 mPa*s

Table 2: AdBlue physical and chemical properties [6]

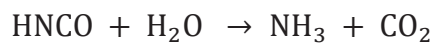
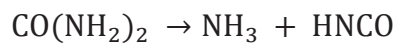
AdBlue has corrosive effects on various metals and must be stored in high quality steels or in plastic tanks, which are preferably used in automotive SCR systems. Another important property of DEF is its high capillarity, which leads to need of precise sealing of entire AdBlue delivery system. Storage tank and delivery lines must be also heated to prevent freezing of the fluid in order to maintain the system operational during low temperature conditions. [1] [2] [4] [5] [11]

2.2 Mechanism of SCR system

AdBlue is delivered from the storage tank into injector and injected directly into exhaust in upstream position to SCR catalyst. This process is controlled by engine control unit (ECU) or Dosing Control Unit (DCU). After reaching exhaust, AdBlue is immediately evaporated and urea is decomposed. This process is described by following hydrolysis reaction:

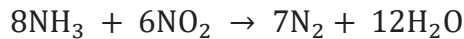
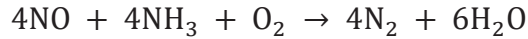


In reality, decomposition of urea is achieved in two steps, where first step is creating intermediate isocyanic acid (HNCO) and one molecule of ammonia by thermolysis of urea. Second step is hydrolysis of HNCO, which leads to products in form of second molecule of ammonia and CO₂. This process is described by following reactions:



Once this process is complete, NH₃ could be used in SCR catalyst, which is great storage media for ammonia. Storage functionality of SCR catalyst greatly improves performance of NO_x reduction by maintaining a steady supply of ammonia regardless to rapid NO_x variations. This storage function has also a benefit in not having to have exactly matched injections of urea corresponding to rapid changing of NO_x levels in exhaust. Urea also could not be injected in temperatures less than 180°C because of hydrolysis kinetics, which is another reason for need of ammonia storage in SCR catalyst during low duty operation. [1] [2] [4]

In SCR catalyst, NH_3 is stored on surface of its catalyst and interacts with NO_x contained in exhaust gas in order to reduce NO_x into N_2 and water via following chemical equations:



„Fast“ SCR reaction: $\text{NO} + \text{NO}_2 + 2\text{NH}_3 \rightarrow 2\text{N}_2 + 3\text{H}_2\text{O}$

Last equation is called “fast” SCR reaction, because it occurs with equal NO and NO_2 and has higher kinetic rate compare to remaining two. SCR systems are also used together with Diesel Particular Filter (DPF) and upstream Diesel Oxidation Catalyst (DOC). Especially DOC can also have beneficial effect on SCR by oxidizing NO to NO_2 via following chemical equation:



This could lead to higher efficiency of some SCR systems, because NO_2 is easier and faster to decompose into harmless products, which was shown on previous “fast” SCR reaction equation. [1] [2] [4] [8] [9]

Schematic description of SCR system is shown on following figure 1.

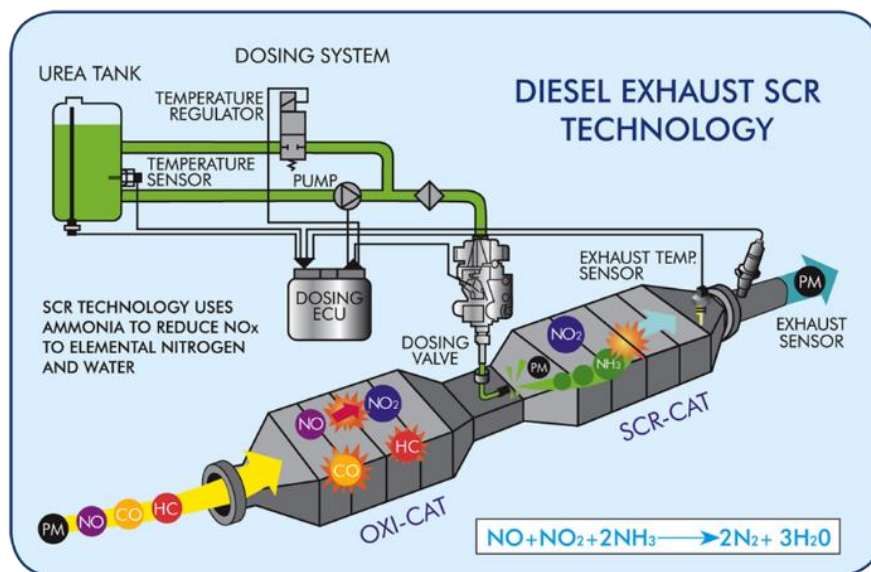


Figure 1: Diesel exhaust SCR technology

2.3 SCR catalyst

Early models of SCR catalyst were composed of vanadium on titanium support. Modern catalyst is composed of zeolite materials with added metals, which are ion – exchanged with zeolite to allow to have its catalytic function. Mostly used metals are iron and Copper.

There are three types of catalyst, which are using different materials:

- Vanadium based catalyst
- Copper – zeolite catalyst
- Iron – zeolite catalyst

Following Figure 2 shows how efficient could be each type of catalyst with respect to the temperature. This behaviour was shown to be the most important decision parameter in step of choosing ideal catalyst for each application. SCR catalyst works under high temperature environment, so Iron – zeolite catalyst is most favoured, because it performs well especially during high temperatures. [2] [10]

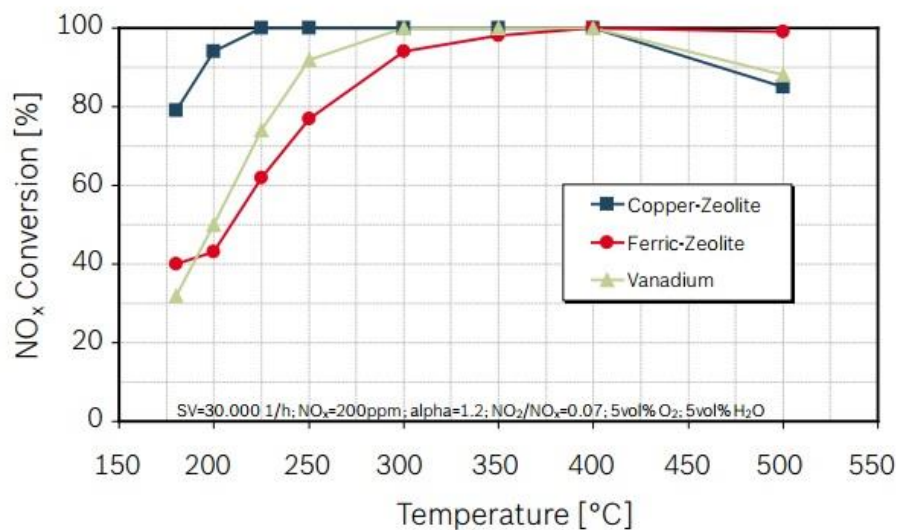


Figure 2: Comparison of different SCR catalyst technologies – NO_x conversion [10]

3 Denoxtronic systems

Purpose of Denoxtronic system is to greatly reduce NOx emissions using SCR technology, which was described in detail in previous chapters. Modern passenger cars with CI engines and common rail system has 95% less NOx emissions compare to typical diesel engines from 1990. After introduction of Denoxtronic system, which was used for the first time in heavy duty vehicles in 2004, there was achieved additional improvement of NOx reduction by 90%. This thesis is focused on mechanical part of DNOx system “Denoxtronic 2.2” produced by Robert Bosch GmbH. Due to this fact, it will be described only Bosch’s Denoxtronic 2.2 system. However, there are additional producers which work on development of this system (such as Nett technologies INC). Denoxtronic system has undergo an intensive development since the first version was introduced to public. [1] [2] [5]

3.1 Denoxtronic 2.2

Denoxtronic 2.2 is a complex system (including urea injection system) for SCR technology introduced to the market in late 2009. It is designed to be used in medium and heavy duty vehicles, but also for some specific off-highway applications. It is achieved 95% reduction of NOx and 3% improvement of engine efficiency by implementing this system into a vehicle. Denoxtronic 2.2 system allow to fulfil EURO V/VI, US10, JPNLT, Tier 4 and Stage 4 emission limits. [5]

3.2 Functional principle of Denoxtronic 2.2

First of all, supply module draws AdBlue from a tank via diaphragm pump. AdBlue is compressed to the pressure of 9 bar, which is needed for proper atomization via dosing module. Pressure is maintained in stable value of 9 bar by controlling speed of electric driven motor of the pump. Task of the Engine control unit or Dosing control unit (depends on type of configuration) is to control dosing, heating and on board diagnosis of the system. Quantity of AdBlue dosing is calculated with respect to several input signals, such as engine load and NOx sensors. Due to the fact that AdBlue has freezing point at -11°C, system must be in ice-free state before becoming operational. This is achieved by using electrical heating or engine coolant. [5] [9]

Denoxtronic 2.2 system consists of:

- Supply module
- Dosing module
- Dosing control unit (optional)
- AdBlue/DEF tank

Scheme of the system and detailed technical information are shown in following figures 3 and 4.

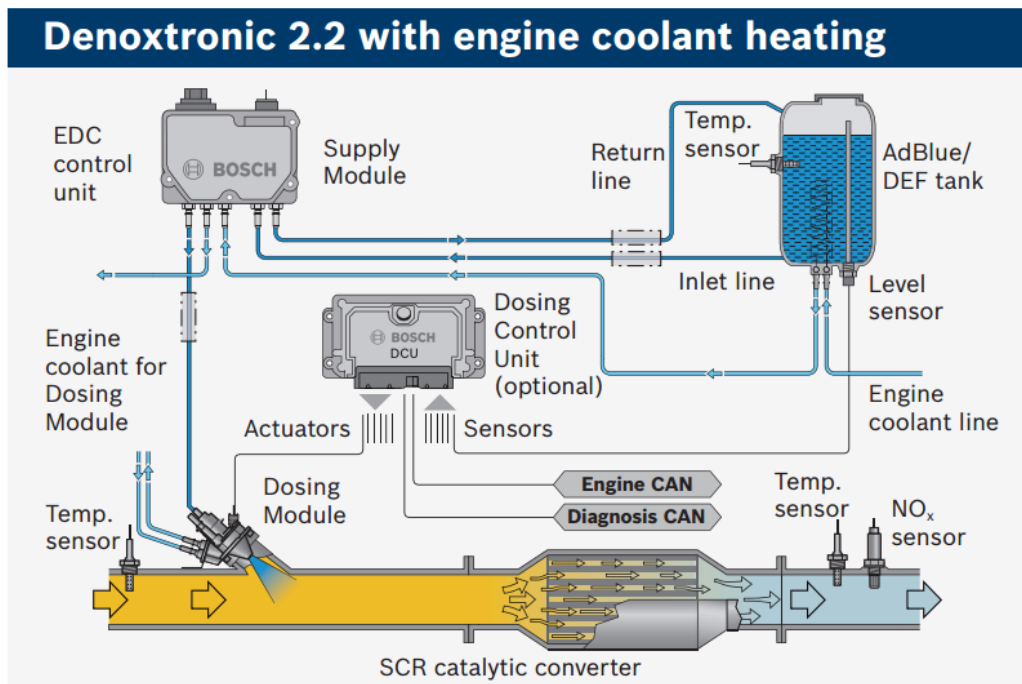


Figure 3: Diagram of Denoxtronic 2.2 system [5]

Technical features	
Dosing quantity (min./max.)	36/7,200 g/h @ 9 bar
Droplet size	≤ 75 μm Sauter Mean Diameter
Lifetime	Equals B10:
Supply Module	30,000 h
Dosing Module	24,000 h
Dosing Control Unit	30,000 h
Start/stop cycles	100,000
Heating concept	Electrical or by engine coolant
Operating voltage	12 V/24 V
Interfaces	
AdBlue/DEF	Plastic SAE J2044 3/8" and 5/16"
Electrical, Supply Module	TYCO 12pin
Electrical, Dosing Module	Bosch compact
Dimensions Dosing Module	L x W x H: 100 x 60 x 110 mm approx.
Dimensions Supply Module	L x W x H: 220 x 209 x 134 mm approx.
Injection line between Dosing and Supply Module: Length	≤ 10 m
Inner diameter	3...6 mm
Fields of application	MD, HD, OHW
Emission target	Euro V/VI, US10, JPNLT, Tier 4, Stage 4

Figure 4: Detailed technical features of Denoxtronic 2.2 system [5]

3.3 Supply module

Task of the supply module (SM) is to build up and maintain pressure of 9 bar in Pressure line to supply Dosing module (DM) with AdBlue under prescribed pressure. Another important function of SM is to fill and empty suction line, Dosing module and hydraulic line during starting and stopping of the system. Residual AdBlue needs to be extracted from supply module before the shutdown of the system in order to prevent damage caused by eventual freezing of residual AdBlue, because AdBlue (similarly to water) increase its volume during transformation from liquid to solid state.

Supply module consists of these components:

- Cover
- Housing
- AdBlue connectors
- Engine coolant connectors (optional)
- Pressure compensation element

- Lead frame
- Filter element
- Equalizing element
- Diaphragm pump
- Magnet
- Pressure sensor
- Reverting valve

You can see the location of each Supply module components on following figure 5.

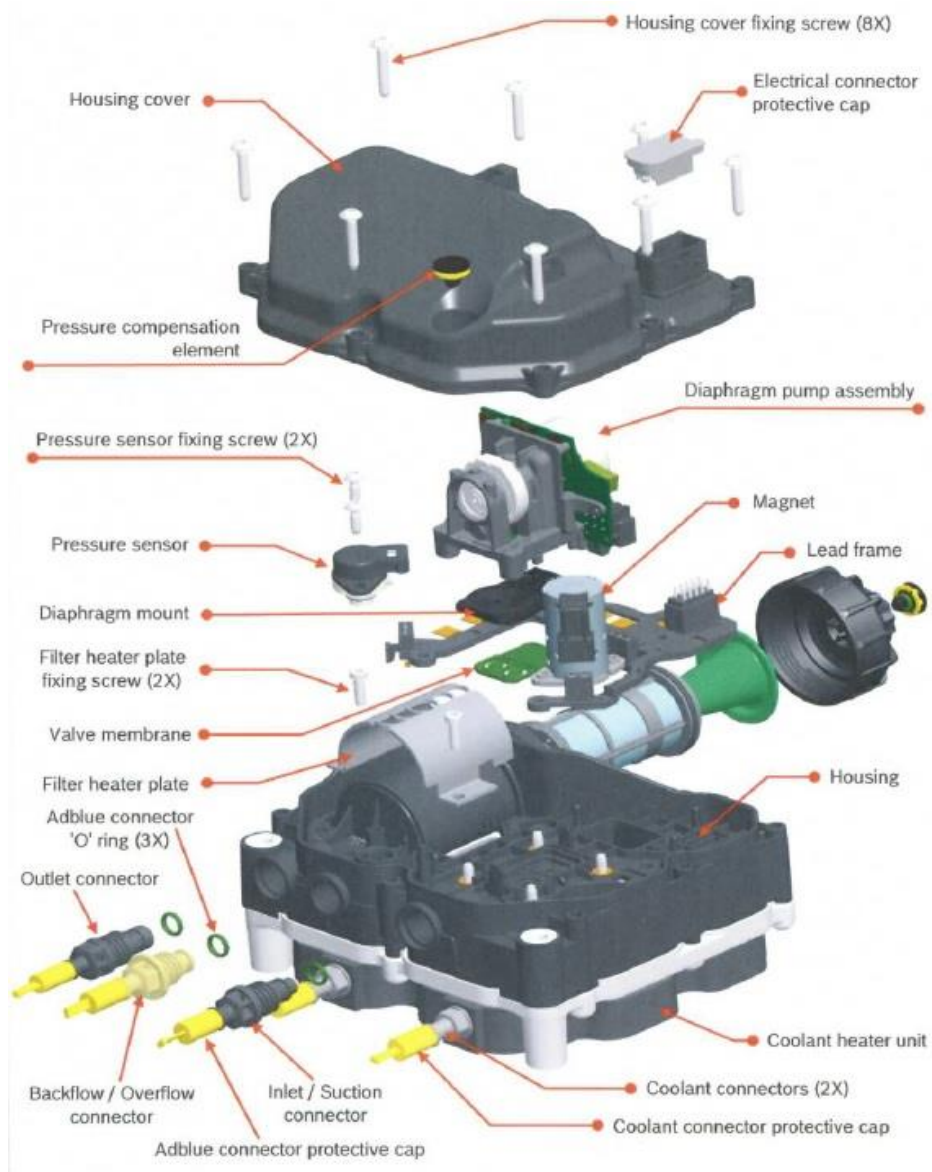


Figure 5: Exploded model of Supply module

We will focus on diaphragm pump, where the membrane of our interest is located. Function of this component will be described in next chapter.

3.4 Diaphragm pump

Main function of this component is to deliver AdBlue solution to Dosing module from DEF tank and vice versa. It is a “positive displacement” pump driven by electric motor. Connection rod (with working membrane attached to the end) of the pump moves up and down. This movement is achieved thanks to the fact that shaft of the pump and connection rod is eccentric. Direction of motor rotation is same for filling and emptying, so 4/2 – way reverting valve is implemented for purpose of changing the direction of AdBlue flow. This Pump is attached via four screws to the diaphragm mount (also known as membrane plate) and housing. Between these two components (diaphragm mount and housing) is placed flexible diaphragm flutter membrane, which will be modelled and examined in this thesis. Flutter membrane could be divided into 2 regions: red region and yellow region (see figure 6)

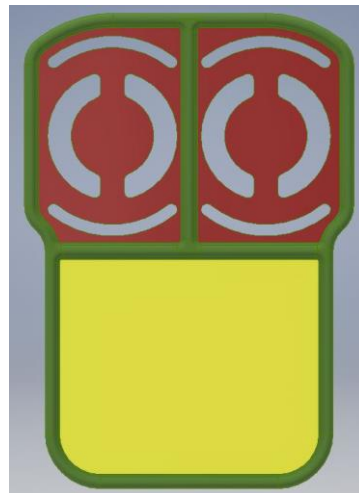


Figure 6: Flutter membrane - region description

Red region is for purpose of opening and closing 1-way inlet and outlet channels via itself deformation generated by differences of pressure made by pump’s working membrane up and down movement. During inlet stroke, pump creates negative pressure in working chamber and cause deformation off flutter membrane which close the outlet port so the AdBlue is sucked into working chamber thought inlet port. During outlet stroke, system behaves vice versa. Working diaphragm moves down and creates positive pressure in the working chamber. This generates positive pressure force on flutter

membrane and deforms it in opposite direction so the membrane closes the inlet port of the pump and AdBlue is forced to exit working chamber through outlet port into pressure line. Yellow region of flutter membrane works as an equalizing element. Under equalizing part of the flutter membrane is located an oscillating chamber. In this chamber is stored small amount of AdBlue which serves as a secondary storage for the pump. During inlet stroke, pump suck out the AdBlue from this oscillating chamber. This causes a deformation of membrane. During outlet stroke, inlet port is closed so the pressure in oscillating chamber is no longer effected by pump. During this period of time, equalizing region of flutter membrane returns to its original shape and during this movement is sucked in small amount of AdBlue into the oscillating chamber so it is prepared for next inlet stroke and whole process could be repeated again. Oscillating chamber is implemented into the system in order to avoid negative effect of inertia and hydrostatic losses in case of AdBlue extraction directly from main storage.

3.5 Material of flutter membrane

This component is made from Hydrogenated Nitrile Butadiene Rubber (HNBR). History of HNBR dates back to late '70s and early '80s when first samples of hydrogenated NBR was developed, however until 1984 was not ready for commercial usage. There were three main companies which stood behind its invention: Zeon Corporation (first company with commercial use of HNBR), Bayer and Polysar. Flutter membrane used in DENOX 2.2 system is made by Datwyler company. [15]

HNBR with Shore A hardness of 80 is type of polymer material with excellent physical and mechanical properties. Main reason for choosing this material is capability to maintain its mechanical properties in wide range of temperature and also because of its resistivity to other chemical substances. This is essential because this part is in most of its operation time in direct contact with AdBue fluid. Basic properties of this material is listed in following table 3. [15]

Color	black
Density	True to sample, +- 0,02 g/mm ³
Shore A hardness	80 (possible change from 0 to +10)
Tensile strength at break	Min. 20 N/mm ² (possible change ± 2 N/mm ²)
Elongation at break	Min. 200 % (possible change from 0 to -20%)

Table 3: Property of HNBR material [16]

4 Description of the problem

DENOX system is not just instantly and immediately operating when we switch on car ignition. The system has to be first filled with AdBlue and then it has to be pressurized to 9 bar to its operating pressure. When the system reaches this pressure, the whole system starts to be fully operational. On the other hand, when we switch off the car, SM has to first drain off the residual AdBlue in order to prevent its eventual freezing under cold climatic conditions. After considering these facts, it was requested to design a test which would simulate (for certain number of repetitions) behaviour of Supply module with focus on period of time when vehicle/DENOX system is being switched on and off. This test will be for purpose of this thesis called as “S/S test” (Start/Stop test). Each customer demand and request for their products certain minimal and safe number of ON/OFF cycles under which will be the system fully operational. For commercial vehicles is this number set to be around 10^5 cycles. This number was defined based on premise that durability of commercial van could be around 15 years and in average could be whole system switched on and off ten times per day. Total number of cycles could be then calculated as:

$$N = Y * D * L$$

$$N = 15 * 365 * 10 = 54\,750 \text{ cycles}$$

Where N = total number of cycles; Y = number of years in operation; D = number of days per one year; L = average number of ON/OFF cycles per day

If we also include the effect of statistical error, possibility of irregularities and also achieving sufficient safety factor, then it was decided to set in general to have already mentioned 10^5 cycles during S/S test. Supply module pass this test when the system is capable to perform all cycles. On the other hand, system fails when SM is not able to finish all cycles. Failed supply module is signaled by its incapability to build up sufficient pressure needed for AdBlue dosing. During this type of test has been in few cases observed signs of damage in way of crack which has been later on propagating through the membrane. This type of damage has not been previously reported from real operation. Due to the fact that this situation could be potential risk it is necessary to determine the cause of damage.

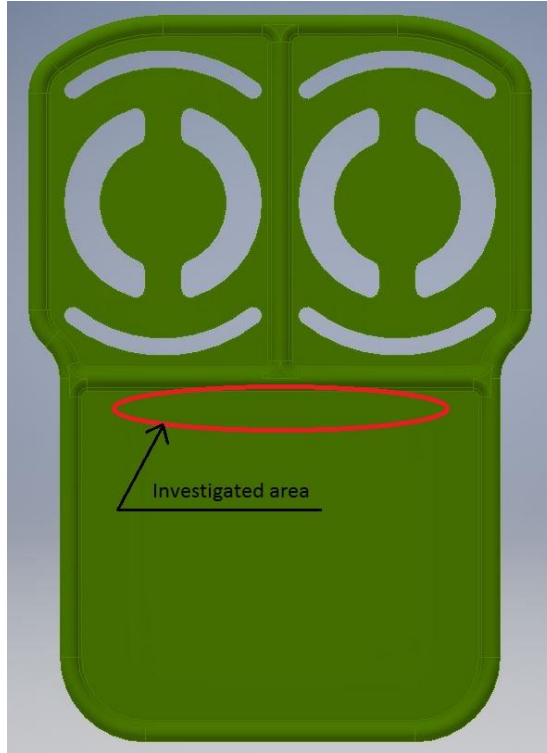


Figure 7: Location of area with highest possibility of crack type failure

Analysis of damaged membranes was assigned to external laboratory where was determined, that damage of the membrane was caused by high mechanical stress of the part and also was proved that the origin of the crack was located on side of the membrane facing to the housing and later on propagated through membrane to the opposite side. Based on these facts I decided to investigate the stress in membrane and also investigate the behaviour of membrane during the S/S test.

4.1 S/S test

In order to investigate the stress of membrane it is necessary to know how the membrane is loaded during the S/S test. Membrane is loaded by pressure differentiation in oscillating chamber during the test caused by pump movement. This pressure in oscillating chamber was measured during one complete cycle by DENOX 2.2 department in RBCB company on transparent model staffed with pressure sensors. Result of this measurement is shown on figure 8 where green line represents the pressure in oscillating chamber.

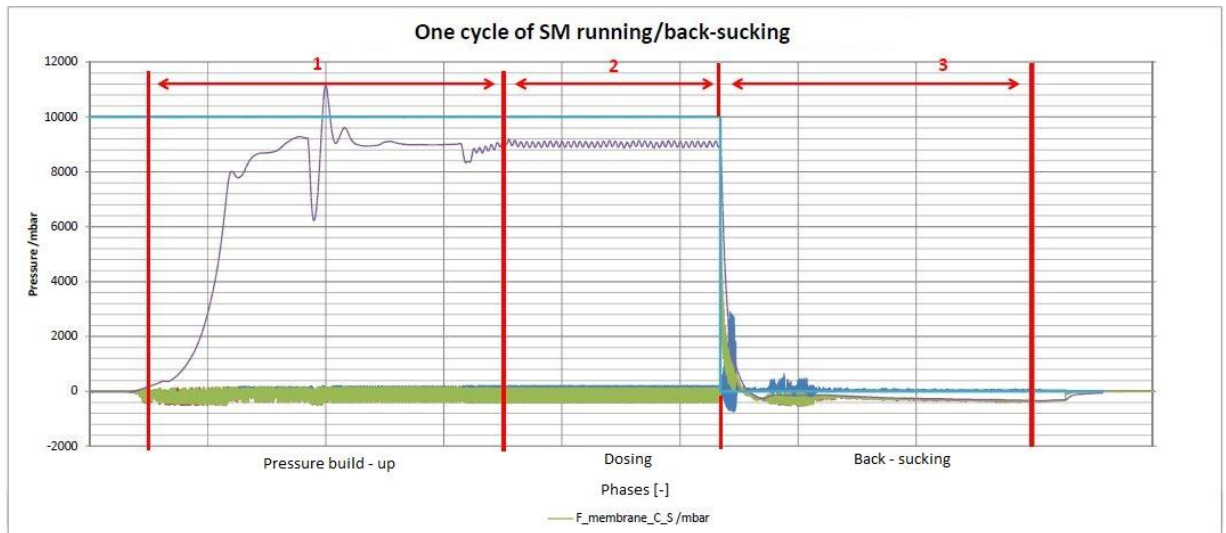


Figure 8: Start stop cycle [16]

4.2 Phases of Start/Stop test

As you can see in figure 8, one Star/Stop cycle could be divided into 3 stages (marked and numbered in red):

- 1) Pressure build-up phase
- 2) Dosing phase
- 3) Back-sucking phase

4.2.1 Pressure build-up phase

Pump starts to operate after acquiring the starting signal send from Dosing control unit (DCU) or Engine control unit (ECU) (depends on type of the system). During this period of time is whole system being filled with AdBlue and is also pressurized for demanded level of pressure. When the supply module achieves stable pressure of 9 bar than the dosing unit starts operate and AdBlue is injected into exhaust gas stream.

During this stage is pressure in oscillating chamber quite stable without any sudden extreme pressure peaks. Pressure oscillation is quite irregular during very beginning of the cycle, however pressure values of irregularities are still within range of maximum and minimum values achieved during steady pressure oscillation. On basis of

this fact I decided not to extra investigate this stage because pressure behaviour in oscillating chamber is basically the same as in consequential phase.

4.2.2 Dosing phase

Pressure in oscillating chamber is regularly oscillating during this phase number 2. Since supply module operates (in real operation) for most of the time under this conditions. I asked RBCB company for values of pressure which could in general approximately represent the pressure changes during dosing phase. I was given sample data which were created only for purpose of this thesis. This data is plotted in following figure 9.

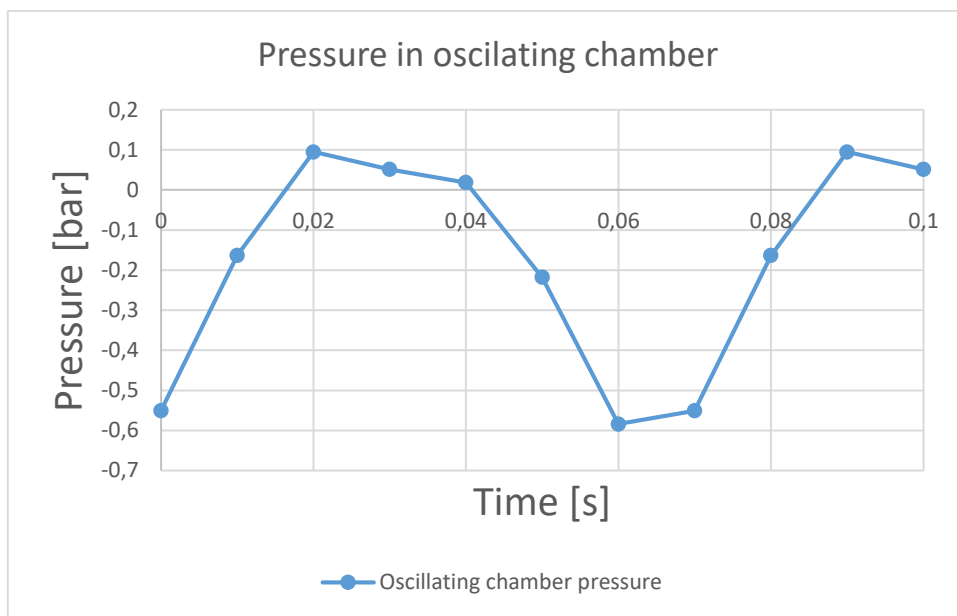


Figure 9: Pressure in oscillating chamber

This pressure oscillation will be simulated and evaluated.

In next paragraph will be described interesting phenomena which occurs when system switch into back sucking phase.

4.2.3 Back Sucking phase

As you can see on figure 8, there is sudden, instant and significant pressure peak right after the system switch from dosing phase to back-sucking. Maximum value of this peak vary from 7 up to 9 bar. This peak is caused by 4/2 reverting valve which causes change of AdBlue flow direction. Function principle of this valve was described in chapter 3.4. Change of direction of AdBlue flow also cause that pressure from high pressure line goes

into oscillating chamber which is part of inlet line. This is the reason of sudden pressure increase. Flutter membrane behaviour under condition of this pressure peak will be also simulated and evaluated.

Dosing stage, where supply module operates at steady and regular conditions for most of the time, is not important during this testing.

5 Identification and validation of material model

It is necessary to choose correct and suitable material model for each type of simulation. This is especially important for hyper elastic materials like HNBR, where the stress and strain curve is highly nonlinear compare to the common materials with linear elastic behaviour (steel, for example). Material testing of rubbers is not only difficult and time consuming process, but there is also high demand for precise and specialized laboratory equipment. I managed to find (with kind help of Ing. Lukáš Franta Ph.D.) laboratory at CTU, where it was possible to test and verify the hyper elastic properties of HNBR material. The testing rig at department of biomechanical engineering was equipped with camera and software for optical strain monitoring directly from marks attached to the sample and not from movement of the clamps. This ability of the testing rig turned out to be very useful and essential, because the ratio of negatively influenced area generated by clamping of the sample to testing rig comparing to whole size of sample was high. After considering this fact, direct clamping, measuring and calculation of the strain directly from movement of the clamps would not be precise and could be misleading.

5.1 Preparation of the samples

For purpose of my measurement, I had to create samples directly from actual flutter membrane product. Due to this fact, I was limited by dimensions of equalizing area of the flutter membrane, where was the biggest area available for creation of the sample.

At a first attempt, I tried to create samples with shapes similar to standardised shapes of testing samples. My aim was to keep sufficient area for clamping and meanwhile still have a sufficient area of the sample where the “width to length” ratio of the sample will be around 10:1. Sample of this shape would be then possible to attach directly to clamps, because the width of the sample in place of clamping would be high enough to avoid sample failure due to high stress generated in area of clamping. After considering what set of equipment was available for me in workshop of BOSCH EDX 2.2 department for creation of these samples, I decided to create 2 versions of sample with shapes and approximate dimensions shown on following Figure. 10.

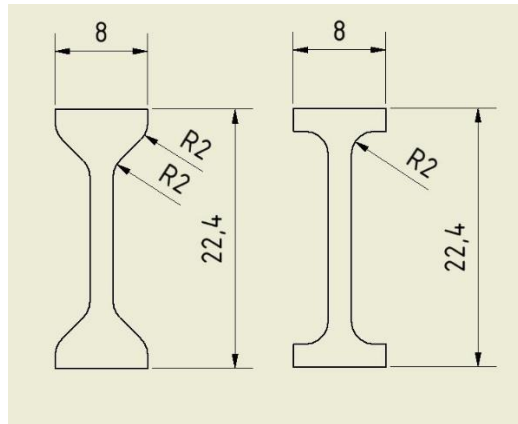


Figure 10: Shapes of samples with approximate dimensions

Both types of samples were made by the same approach: straight sides were cut off by extremely sharp utility knife and radii were cut out by dies with corresponding dimensions by use of sharp scalpel.

This approach turned out to be inconvenient due to this reasons:

- It was impossible to achieve precise radii by using die due to the small dimensions of the sample. One of the reason was that outer dimensions of the die was in collision with rims of the sample.
- Tangential connection of straight and curved edges was imperfect.
- Samples were visually unsymmetrical by both axes.
- Width of the area dedicated to optical strain measurement was not constant through the whole length of this area.

Using this type of specimen would lead to inaccurate measurement and there would be high probability that the sample fails during testing. Considering the fact that my time available for measurement was only one day and not even whole, I could not afford failure and repetition of the test.

After this troubles with complicated shape of sample, I decided to sacrifice wider area for clamping in order to create simple samples with constant width and smooth edges through whole length. In order to avoid high change of sample width during measurement I decided to keep the “width to length” ratio around 1:10. 3D shape and approximate dimensions of the sample are shown in following figure. 11.

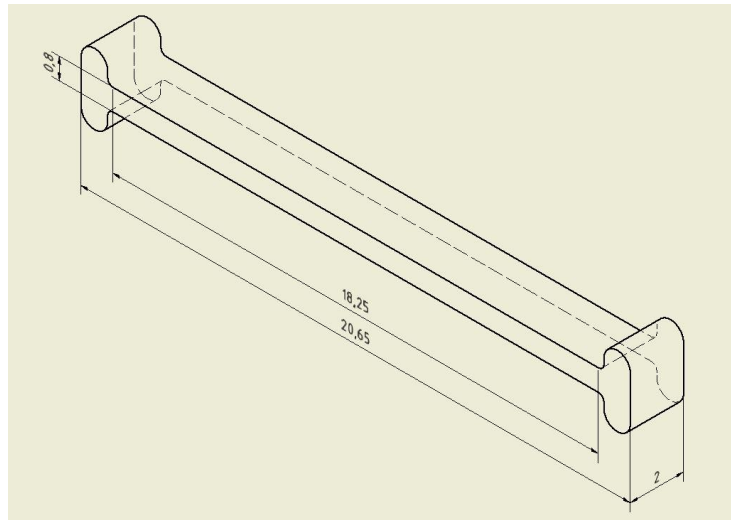


Figure 11: Final shape of samples

Each sample was taken from unique final membrane product. Half of the samples were taken in “X” direction and the second half from “Y” direction. I choose to create two sets of samples in both axes in order to check if the behaviour of material is independent to its orientation. Evaluation and result of this hypothesis will be stated further on.

At first, I created 8 samples – 4 in each direction. Samples were divided into 2 sets called “short” (Location 2 – “Y” direction) and “long” (Location 1 – “X” direction) corresponding to their length. Location of place where the samples were cut out are shown in following Figure 12.

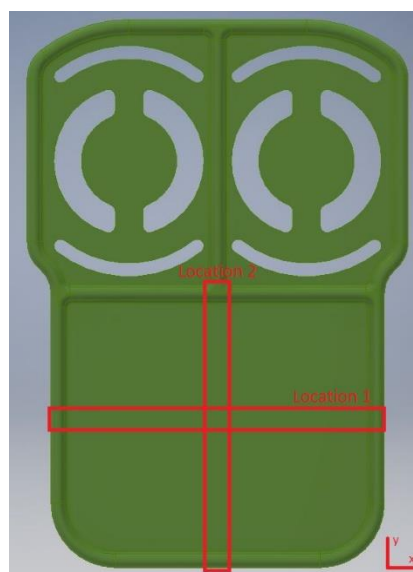


Figure 12: Locations of cuts

Criteria for selecting the best samples were:

- There was no sample damage after visual check. If the sample was damaged, than it was excluded from experiment.
- Each visually OK sample was measured in 3 points: in the middle and at the opposite ends. The most accurate samples were identified as the samples with smallest standard deviation of sample width.

Dimension of the width was measured in RBCB investigating laboratory on microscope measurement gauge connected to the computer. It was taken picture of each sample and each width was measured by using software ruler tool (see Figure 13). All pictures could be found enclosed on CD.

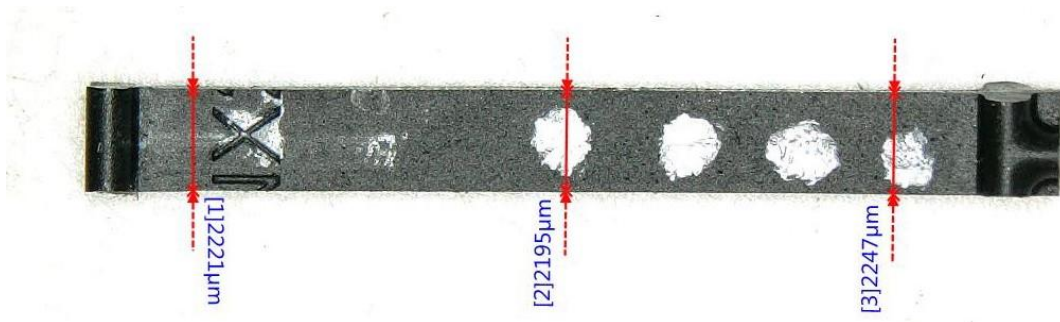


Figure 13: Real sample measuring on microscope with software ruler

Summary of this measurement is in the following Table 4

Sample Number	1S	2S	3S	4S	1L	2L	3L	4L
1st dimension [mm]	1.72	1.99	2.04	2.25	1.72	1.86	2.07	2.14
2nd dimension [mm]	1.80	1.91	2.09	2.20	1.80	1.80	2.09	2.09
3rd dimension [mm]	1.80	1.96	2.12	2.22	1.85	1.83	2.09	1.93
Avg. dimension [mm]	1.77	1.95	2.08	2.22	1.79	1.83	2.08	2.05
Thickness [mm]	0.80	0.80	0.80	0.80	0.80	0.80	0.80	0.80
Cross-section [mm ²]	1.42	1.56	1.67	1.78	1.43	1.46	1.67	1.64
Standard deviation	0.05	0.04	0.04	0.03	0.07	0.03	0.01	0.11

Table 4: Samples dimensions and evaluation - first set

After overall checking of the dimensions, I found out that pool of 8 sample is insufficient for choosing the most quality sample. Due to this fact, I made another 10 samples – 5 in each direction and evaluated them by the same way as previous 8 samples

and create second table for new 10 samples. The only difference was that microscope with software ruler was no longer available for me. After consultation with Mr. Chlup (supervisor of physical measurement at CTU) we decided that it is not necessary to measure the dimensions on microscope and measuring by using sliding scale with accuracy to 2 decimals will be sufficient for purpose of this measurement. Results of this measurement is listed in following Table 5.

Sample Number	1S	2S	3S	4S	5S	1L	2L	3L	4L	5L
1st dimension [mm]	2.45	2.12	2.50	2.51	2.55	2.00	2.33	2.53	2.38	2.66
2nd dimension [mm]	2.40	2.10	2.50	2.55	2.63	2.02	2.44	2.42	2.33	2.62
3rd dimension [mm]	2.34	2.10	2.53	2.68	2.67	2.01	2.52	2.51	2.24	2.53
Avg. dimension [mm]	2.40	2.11	2.51	2.58	2.62	2.01	2.43	2.49	2.32	2.60
Thickness [mm]	0.80	0.80	0.80	0.80	0.80	0.80	0.80	0.80	0.80	0.80
Cross-section [mm ²]	1.92	1.69	2.01	2.06	2.09	1.61	1.94	1.99	1.85	2.08
Standard deviation	0.06	0.01	0.02	0.09	0.06	0.01	0.10	0.06	0.07	0.07

Table 5: Samples dimensions and evaluation - second set

To summarize this, there was available in total 18 samples – 9 in each direction. Based on the data I selected 4 most accurate samples in each direction. These samples are marked green in the previous Table 4 and Table 5.

Photograph of this new set of samples ready to be tested with their new designation could be found in following Figure 14. Samples number 0 are designated to be checking samples for validation that testing rig is properly adjusted and so these samples are not covered in results.

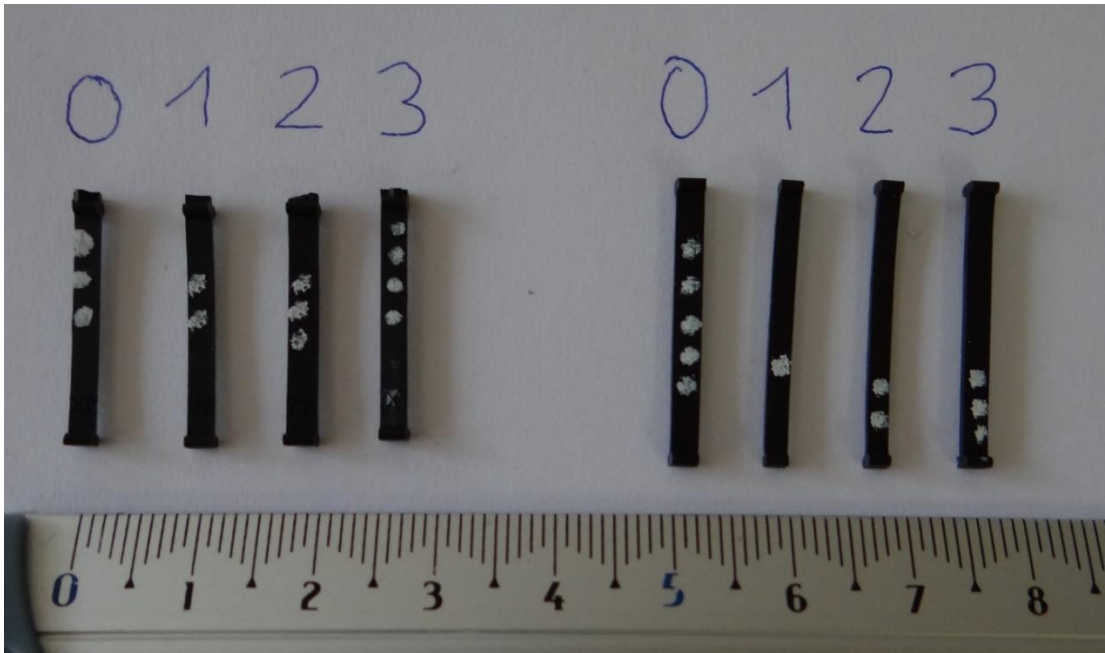


Figure 14: Set of samples prepared for testing

After having samples ready for testing it was necessary to solve the problem of attaching the sample to the clamping forceps of the testing rig. Samples of approximately 2 mm width could not be directly clamped to the test rig because size of the forceps was too big compared to the size of the sample.

I designed an additional tool which solved this problem. I used side rims of the sample as area where the force generated during testing will be transmitted from forceps to the sample. This tool was made from 2 aluminium parts whose stiffness is order of magnitude higher than stiffness of the HNBR. Then the tool may be considered as rigid. For 3D model with important dimensions see following Figure 15.

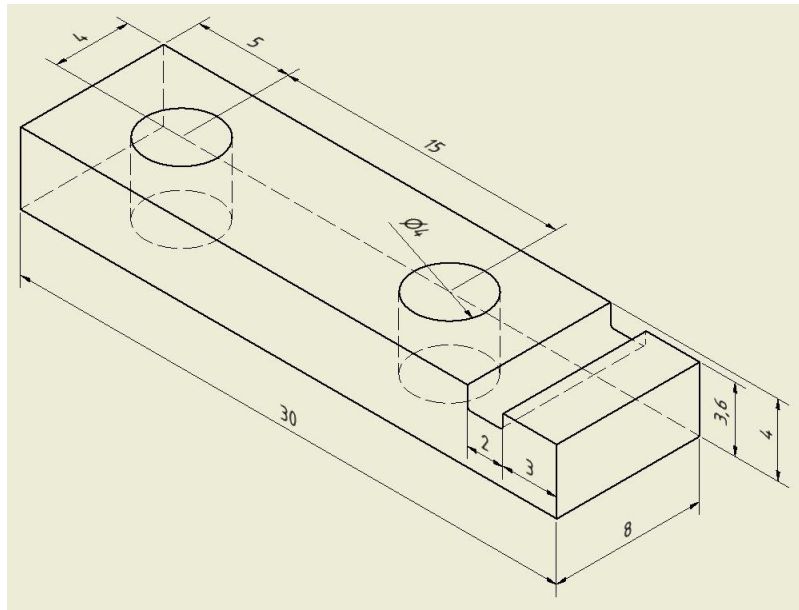


Figure 15: Model of aluminium tool with general dimensions

Tools were created (made from 4 parts) based on my 3D model with kind help from Mr. Ficko (milling machine operator) by using a milling machine located in DNOX 2.2 department. In addition, edges of the tool in contact with sample were smoothed by file and there was also created metric thread for purpose of bolt connection.

5.2 Procedure of sample connection to the tool and testing rig

First step: Preparation of the sample

Sample is prepared for the test after adding small piece of paper which covered the area of tool and sample contact (see following Figure 16). I decided to add the piece of paper because the faces of the tool were not very smooth. I verified by simple tension test in my bare hands that if I add the paper the contact is better and sample remain seated in aluminium tool.



Figure 16: Prepared sample with paper attached

Second step: Assemble the sample with the tool

Sample is fixed to the tool by frictional force generated by compression force. This compression force was generated from bolt connection. This assembly is shown in following Figure 17, Figure 18 and Figure 19.

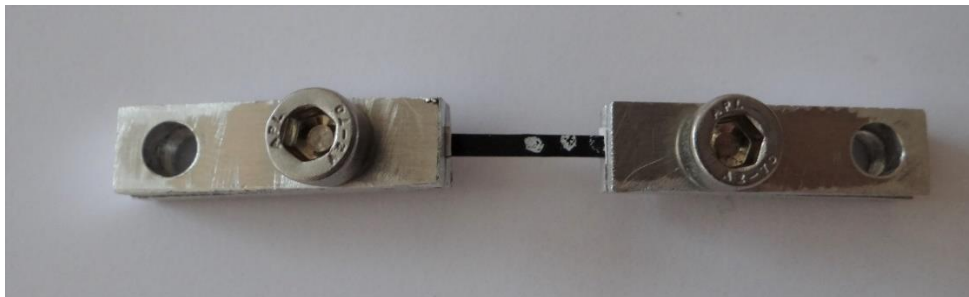


Figure 17: Sample assembled with tool - top view



Figure 18: Sample assembled with tool - side view

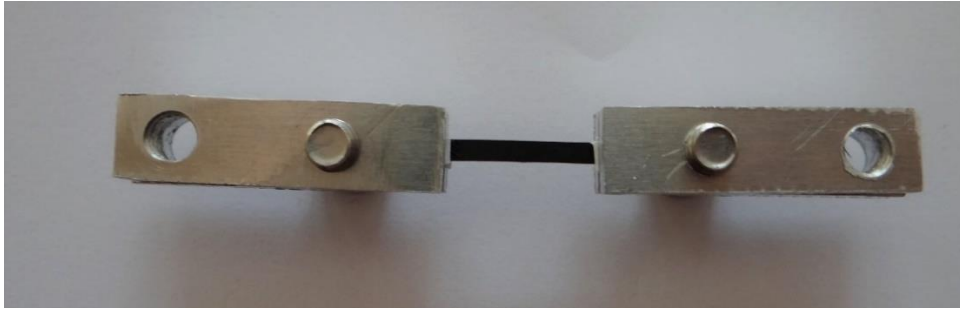


Figure 19: Sample assembled with tool - bottom view

Third step: mounting to the testing rig

Forceps were removed from testing rig, because they were no longer needed. Connection between tool and testing rig was achieved by using bolt as a pin which went through tool and the testing rig. Pictures of this final assembly are shown in following Figure 20 and Figure 21.

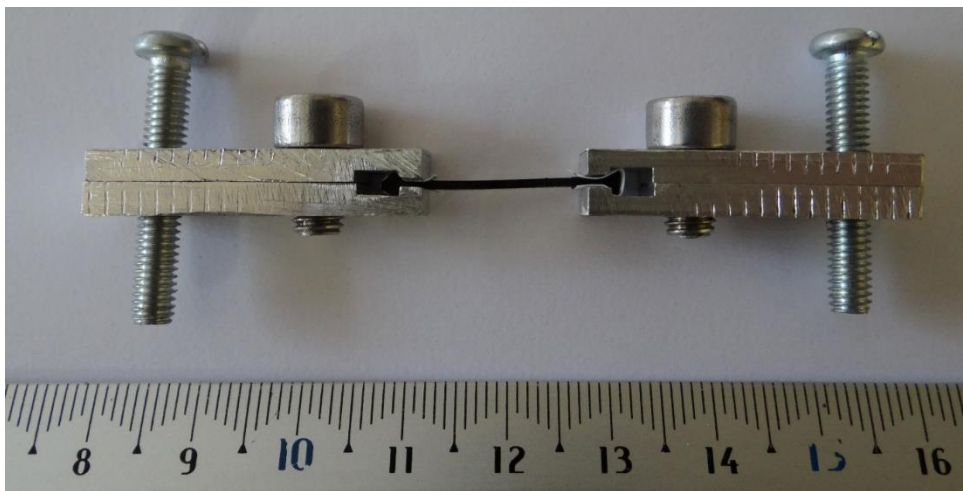


Figure 20: Assembly prepared to be attached to the testing rig

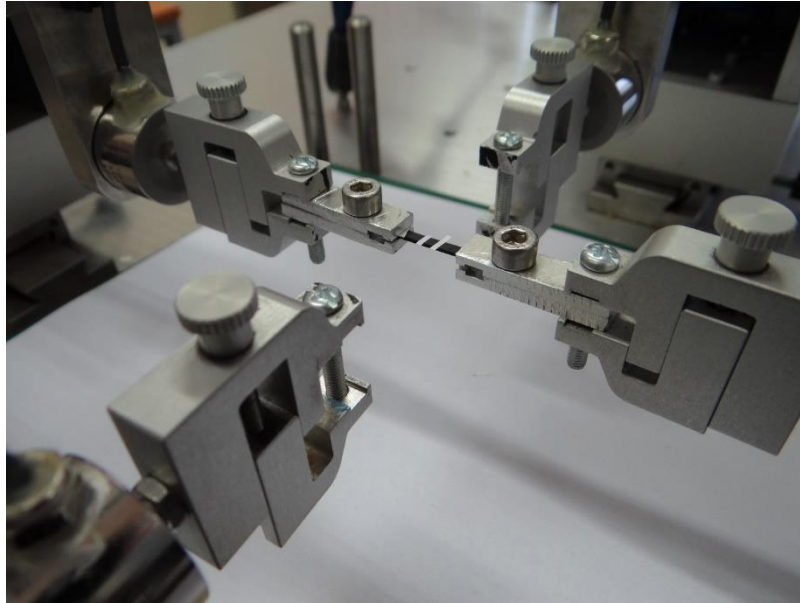


Figure 21: Sample with marks attached to testing rig - ready for testing

Advantage of having this type of connection instead of clamping the tool directly between the forceps is that this type of connection allows rotational movement around axis of the pin. Thanks to this fact, whole assembly could self-align at the start of the test and thus avoid creation of additional stress made by imperfect mounting.

In this step we also attached control marks to the sample for purpose of optical strain measurement. Marks were made from small pieces of white paper sticker placed in the middle of the sample with approximate distance of 5 mm. Value of distance between the marks does not have to be always the same, because we set the camera individually for every sample. Principle of how this optical measurement works will be ideally described by following Figure 22, where black component is measured sample, grey components are tools and thick white lines are marks.

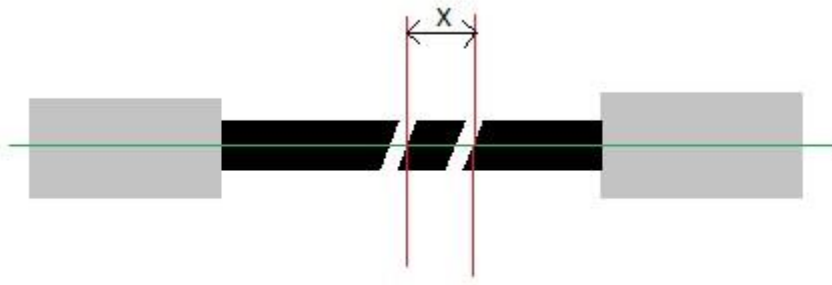


Figure 22: Optical strain monitoring and measurement

Camera captures the whole sample during the test. This record is shown live on PC where is post processed by software where user can see the same as was shown in previous Figure 22. Software can find an area where is a sudden change of colours. In this case, we manage to have optimal colour change from black (colour of the sample) to white (colour of the marks). In order to obtain only one specific point which will be monitored, we define a line (green line on Figure 22) in software where the program automatically find this specific points. Now we have 2 points (on Figure 22 are represented by crossings of green and red line) and their position and movement is followed and recorded.

After having he sample connected with testing rig we manually adjust the position of the arms of the testing rig in order to set the sample almost to the state where tension is approximately zero (small pre-tension offset was allowed). Now the sample is ready for measurement.

6 Physical measurement

After few attempts with spare samples we set the parameters of the test. Sample will be loaded via arm movement – each one in opposite direction. Generated force will be measured by load cells installed in testing rig with maximal range of 200 N. Movement of each arm was set to 10 mm for shorter samples and 12 mm for longer samples. These values were determined in order to achieve approximately true strain of 70 percent.

As an output of this measurement we get a file in .xls format, where are stored sets of data in respect of time. This data is:

- Time [s]
- Absolute position of crosshead 3 (M3) and 4 (M4) [mm] (crosshead 1 and 2 is inactive in this testing)
- Relative position of crosshead 3 (R3) and 4 (R4) [mm]
- Force on load cell 3 (F3) and 4 (F4) [N]
- Distance between markers (X) [mm]

After collecting these data, I did manual post-processing of this data in order to get stress strain curve for each sample.

6.1 Data post-processing

If we want to obtain Stress-Strain curve, we need to calculate true strain and true stress. These values cannot be calculated directly from data acquired during measurement. It was necessary to calculate for each time step these data:

- Mean Force [N]
- Nominal cross-section of sample (A) [mm²]
- Nominal Strain [–]
- Nominal Stress [N/mm²]
- True Strain [–]
- True Stress [N/mm²]

Mean Force

Calculated as mean value of F3 and F4

$$\text{Mean Force} = \frac{F3 + F4}{2} \text{ [N]}$$

Nominal cross-section

This value was already calculated and listed in Table 4 and Table 5.

Nominal strain

$$\text{Nominal strain}_t = \frac{X_{t+1} - X_0}{X_0} \text{ [-]}$$

Where:

X_{t+1} = *distace between markers in next time increament*

X_0 = *initial distance between markers during start of the testing*

This approach is valid, because data was recorded in rate of 20 Hz (20 data samples for 1 second of measurement) so the time increment difference is very low and thus the error of this computational approach is minimal.

Nominal Stress

$$\text{Nominal Stress} = \frac{\text{Mean Force}}{A} \text{ [N/mm}_2\text{]}$$

True Strain

$$\text{True strain}_t = \ln(1 + \text{Nominal strain}_t)$$

True stress

$$\text{True stress} = (1 + \text{Nominal strain}) * \text{Nominal stress} \text{ [N/mm}_2\text{]}$$

All previously mentioned data was calculated by using MS Excel program, where this vast set of data could be easily post-processed. This measured and calculated data for all samples could be found in enclosed CD.

As a result of this post-processing is set of 6 Stress-Strain curves. These curves are shown on following Figure 23.

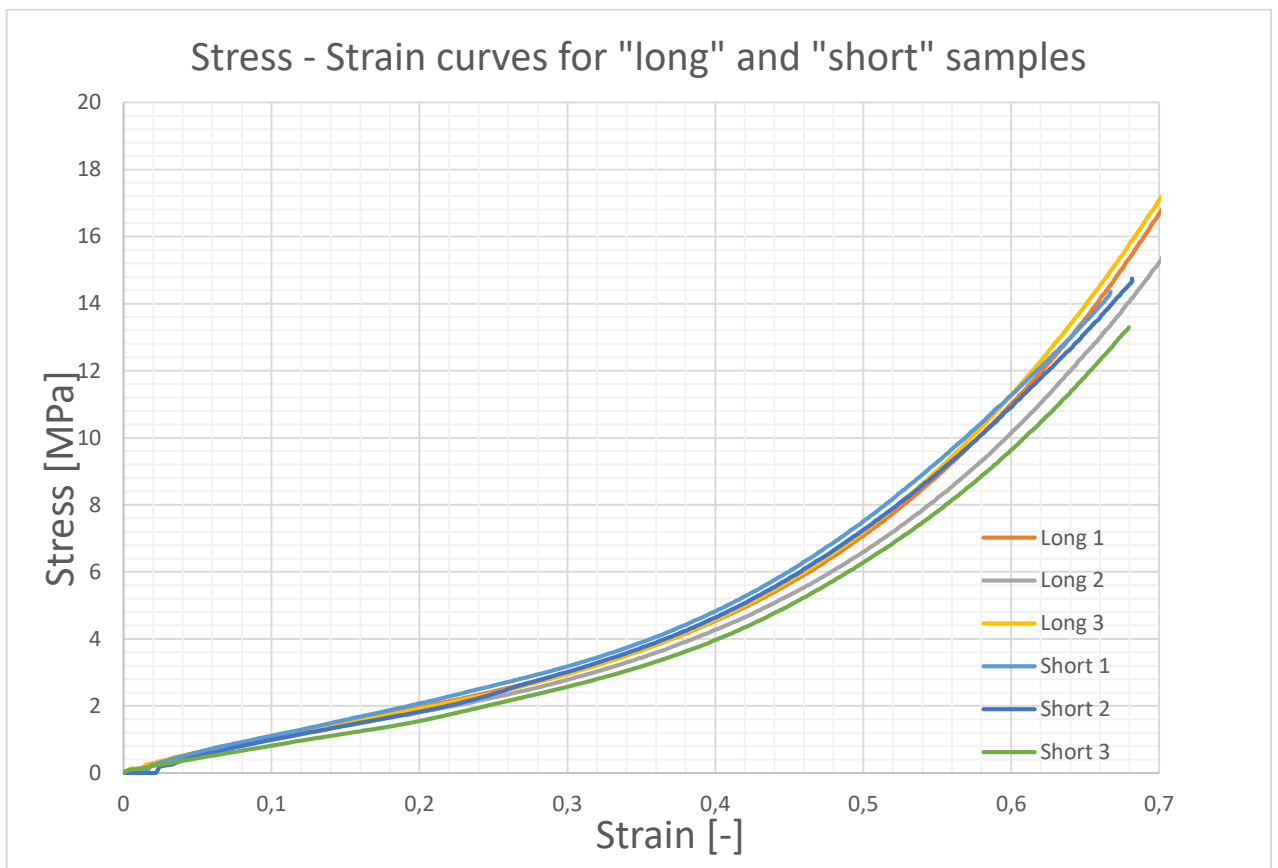


Figure 23: Stress strain curves for all measured samples

6.2 Result of measurement

There was no severe difference between each sample in set of “short” samples except sample “Short 3”. Sample number “Long 2” in set of “long” samples differs a bit from samples “Long 1” and “Long 3”. These differences could be caused by irregularities of the samples and error of measurement. Sudden and random changes of the Stress during early start of the test was due to imperfect seating of the sample in aluminium tool. This noise disappeared after achieving ideal seating and no longer negatively affect the measurement. However, if we look at the result we can in general say that all curves have the same characteristics.

7 FEA simulation of physical measurement

In order to verify accuracy of hyper elastic material models with actual data, I simulate this testing in ABAQUS CAE software. In each module, there was set these properties.

7.1 Simulation settings

Part

Testing samples (one in each direction) was cut off from 3D model of membrane product in the same spot as in real measurement. Width was set to 2 mm. I used Inventor SW for this procedure and final testing sample was exported to STEP file and after that imported to ABAQUS CAE as 3D deformable body. Also dimensions of sample were checked by the “Query” tool for verification that the dimensions are in orders of millimetres.

Property

I created in “Material manager” card two materials with different Neo Hook models and one material with Yeoh material model

1st model: Neo Hook

These constants were obtained from material data card created by Robert Bosch company material testing centre. Constants for this model are:

$$C_{10} = 0,6414 \text{ MPa}$$

Incompressibility parameter $D1 = 0,001 \text{ MPa}$

2nd model: Neo Hook – estimated

Constants of this model were estimated from Briscoe formula with use of knowing Shore A value.

Briscoe formula:

$$G_{\infty} = 1,15 * \frac{5,527 + 0,7167 * Shore A}{2 * (100 - Shore A)}$$

$$C_{10} = \frac{G_{\infty}}{2}$$

If we input value of Shore A = 80, we could calculate C10 constant which is used in ABAQUS SW. For comparison, ANSYS SW works with G_{∞} value.

$$G_{\infty} = 1,15 * \frac{5,527 + 0,7167 * 80}{2 * (100 - 80)} = 1,8073$$

$$C_{10} = \frac{1,8073}{2} = 0,9037 \text{ MPa}$$

Incompressibility parameter $D1 = 0,001 \text{ MPa}$

3rd model: Yeoh

These constants were obtained from material data card created by Robert Bosch company material testing centre. Constants for this model are:

$$C_{10} = 0,4795 \text{ MPa}$$

$$C_{20} = -0,2206 \text{ MPa}$$

$$C_{30} = -0,1685 \text{ MPa}$$

Incompressibility parameter $D1 = 0,001 \text{ MPa}$

All other properties of this material models except previously mentioned hyper elastic properties could be found enclosed on CD in ABAQUS material data cards.

Assembly

There is only one part in this simulation, so there was not any operation in this module.

Step

For this testing, I used “Visco” step with modifying these options:

- Time period = 50 s
- Nlgeom = ON
- Increment size [s] = 0,1 initial; 0,005 minimum; 0,5 maximum
- Creep/swelling/viscoelastic strain error tolerance = 0,02

Time period was calculated from velocity of arm movement and distance of the arm needed to be displaced.

$$T = \frac{x}{v} = \frac{10}{0,2} = 50 [s]$$

Where: x=distance of the arm needed to be displaced; v= velocity of arm movement

Interaction

There was no need for adjustment – no interactions take part in this simulation

Load

For description of loading see following Figure 24.

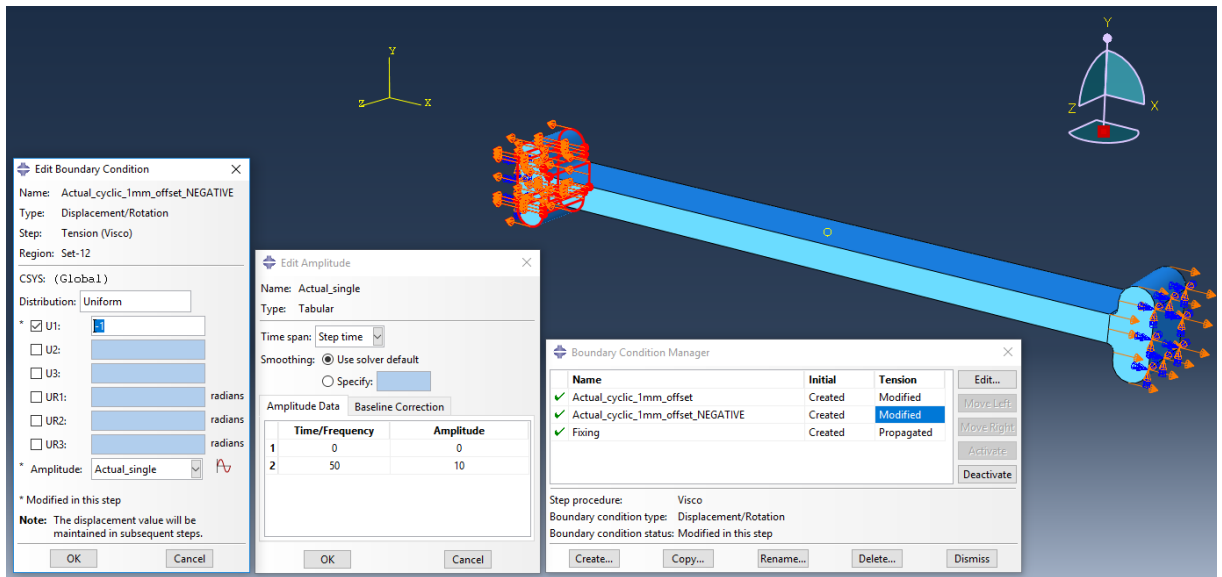


Figure 24 ABAQUS simulation - Load settings

Sample was loaded in simulation by same way as in real measurement with one difference that each arm displacement (on both sides) was transformed to the sample via cells made from rim part of the sample. This caused that during simulation there was not generated initial sliding and deformational error (disturbance) which was measured during real measurement (already mentioned in chapter 6.2.).

Movement of each arm was controlled trough “Amplitude” option, where was displacement linearly distributed through the whole period of simulation.

There was left only one degree of freedom in “X” axe for both cells where loading is applied by using “Fixing” BC, where faces at each end of cell were constrained in all DOF except U1 (“X” axe).

Mesh

Part was meshed by using C3D8RH element: An 8-node linear brick, hybrid, constant pressure, reduced integration, hourglass control. See Figure 25.

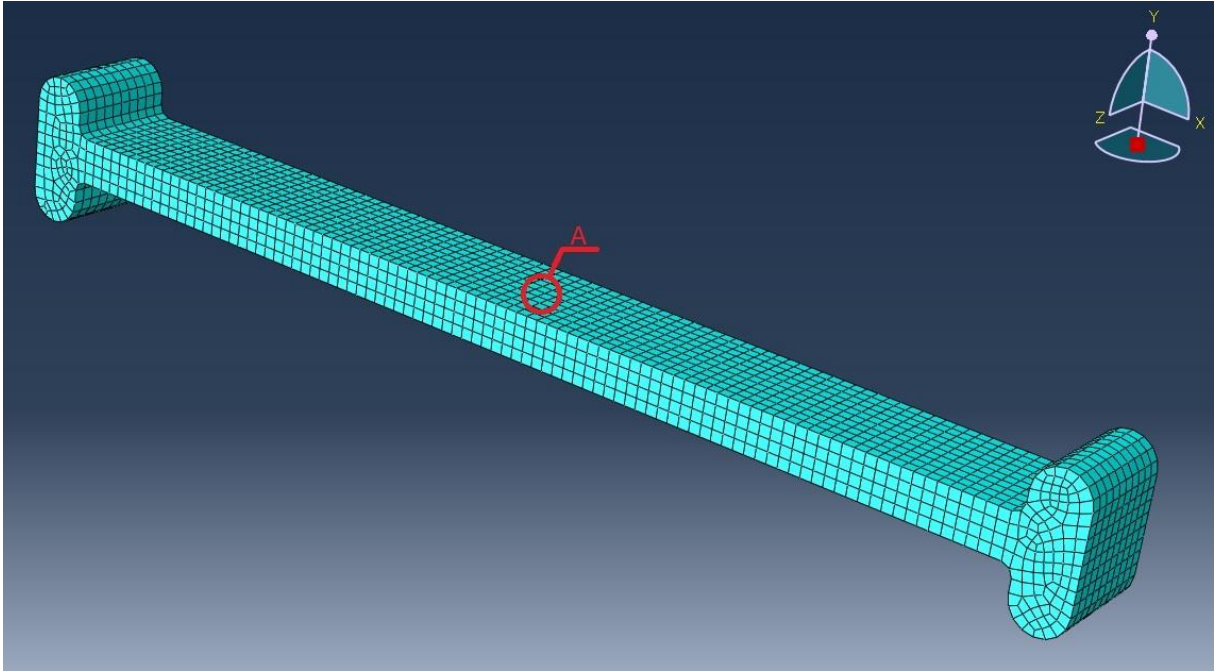


Figure 25: Meshed sample with C3D8RD elements

Mesh was verified with 0 error and 0 warning elements.

After this step, I proceeded to creating and submitting the job for each material model created in “Property” card. This simulation was successfully completed for all material models and also for “short” and “long” sets. For creation of interpreting data, I choose one element located in area “A” and for this element I extracted its data for Strain in “X” direction (LE11) and data for Stress in “X” direction (S11). There are also implemented Stress – Strain curves obtained from real measurement for purpose of comparison the accuracy of models. This data is plotted in following Figure 26 and Figure 27.

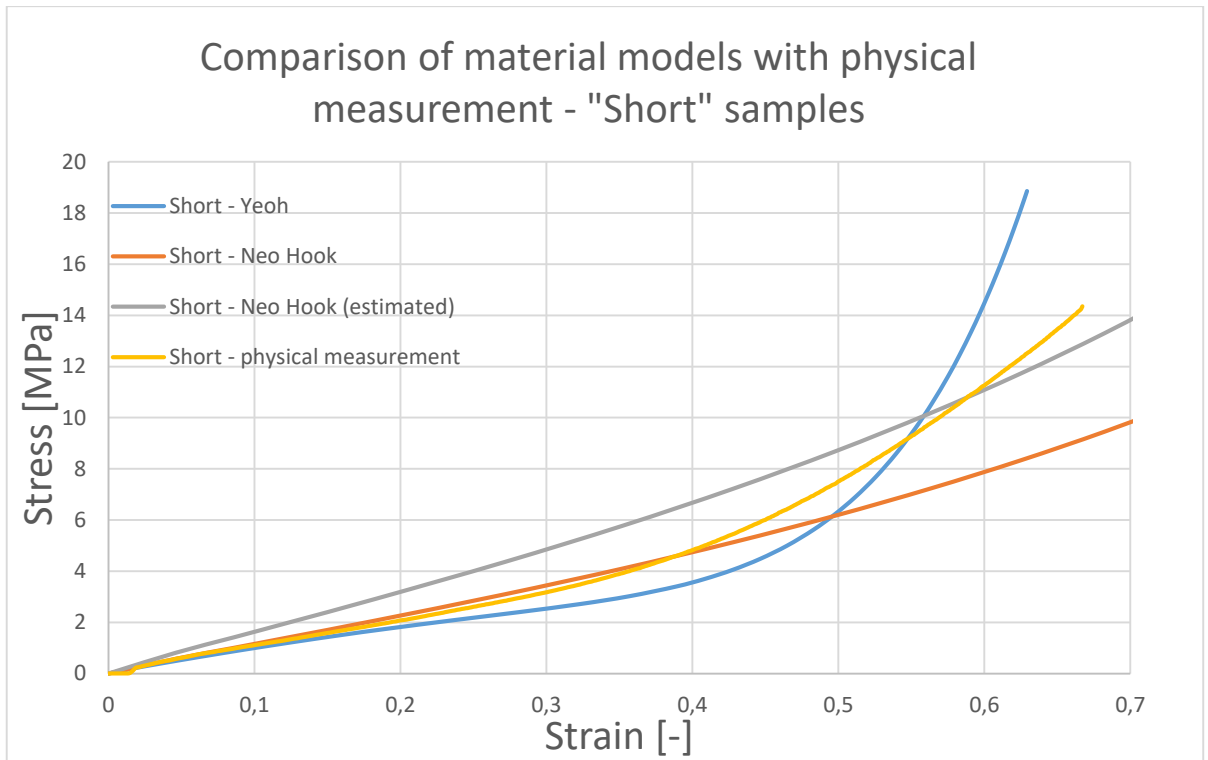


Figure 26: Comparison of material models with real measurement on short samples

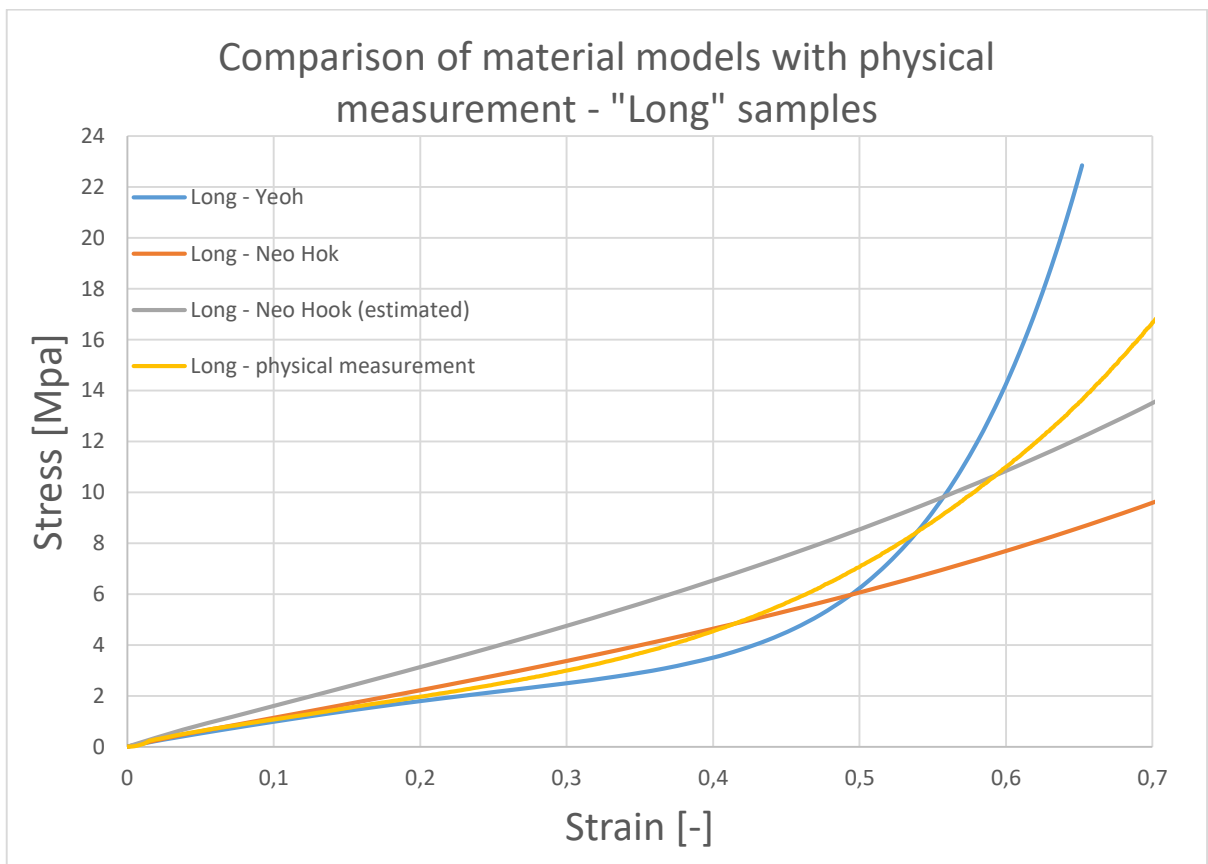


Figure 27:: Comparison of material models with real measurement on long samples

7.2 Comparison of stress strain curves from simulation and measurement

We can see in previous Figure 26 and Figure 27 four stress strain curves – three curves from simulations of different material models are compared to stress strain curve obtained from physical measurement.

We could state from this charts, that:

- “Neo Hook” material model is more accurate than “Neo Hook – estimated” model.
- “Neo Hook” is the most accurate model in range from 0 % to approx. 40 %. This model starts to be very inaccurate when strain is higher than 40 %.
- „Yeoh“ material model is quite accurate and could be also used until strain of approximately 25%. However, this model is less accurate in residual range of strain.

After considering the results, “Neo Hook” represents the best actual material properties and so this material model could be chosen to be main material model for further simulations under condition, that strain during these simulations will not exceed 40%.

After material model validation, I proceeded to 2D and 3D flutter membrane physical stress simulation.

8 FEA simulation of real and modified designs

As it was mentioned in chapter 4, from crack analysis of real sample made by external company it was determined, that the crack was initiated due to the high stress generated during operation. I decided to build a hypothesis on this and analyse the stress of the membrane during these 3 modes of operation:

- Regular cycle during dosing
- Switching off phase with overpressure peak of 7 bar (0,7 MPa)
- Switching off phase with overpressure peak of 9 bar (0,9 MPa)

Each mode of operation has its own specific properties which has been set.

Part

From 3D model of whole assembly, I extracted only 3D model which goes through the housing, flutter membrane and membrane plate in location of oscillating chamber, so basically cut view of oscillating chamber is generated (see Figure 28).

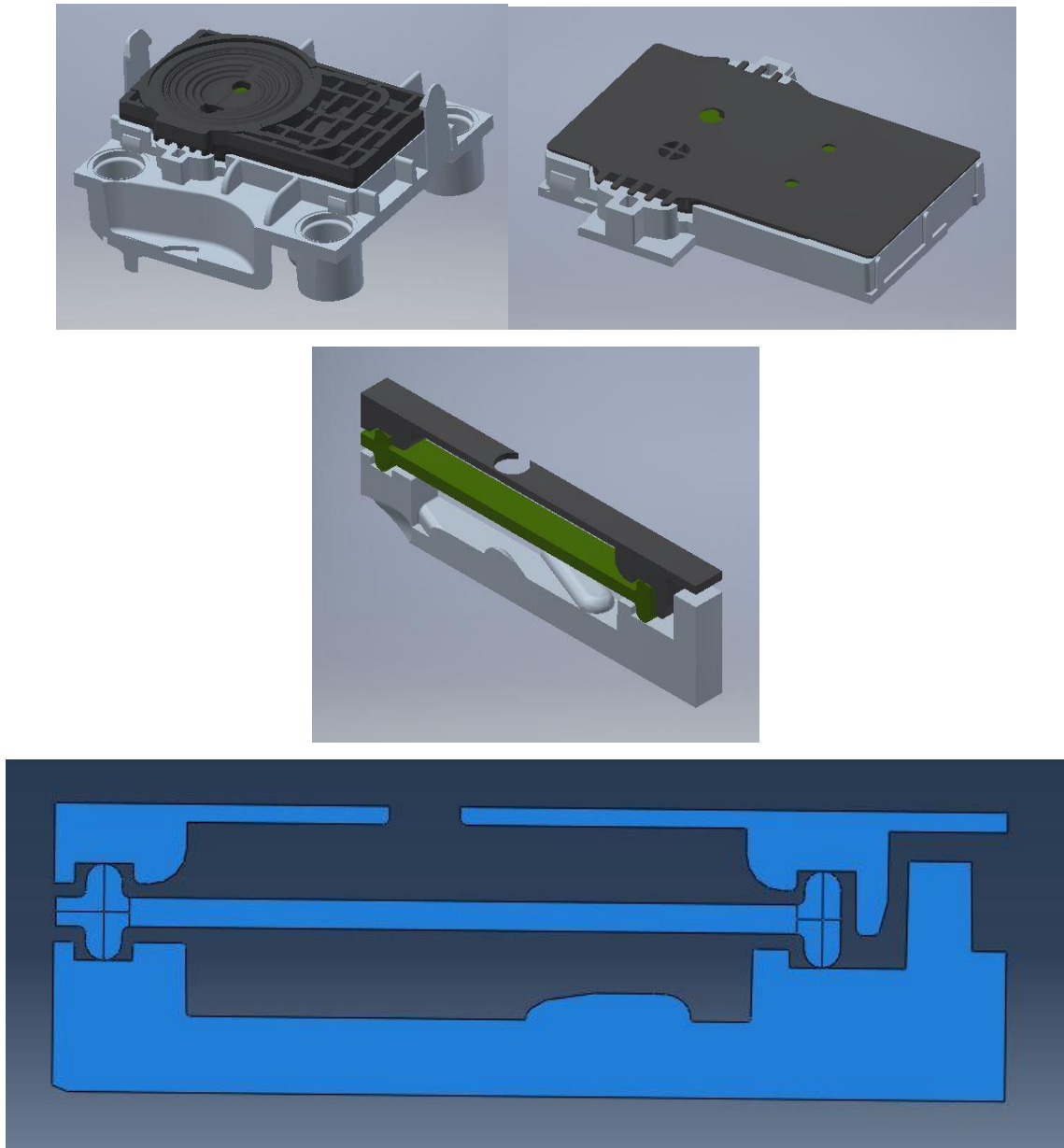


Figure 28: Steps of 2D model creation

2D model was imported into ABAQUS as 2D deformable set of parts with scale multiplication of 1000 in order to maintain dimension's values in units of millimetres. This was checked by Distance tool (Tools – Query – Distance).

Property

As it was mentioned before I decided to use Neo Hook material card provided by BOSCH company, so I defined and assigned for flutter membrane HNBR material with Neo Hook hyper elastic behaviour. These material cards could be found on enclosed CD in form of .txt files.

Considering the fact, that housing and membrane plate have robust design, and they are made from plastic material which has stiffness in orders higher than HNBR, I decided to look at housing and membrane plate as non-deformable bodies. In order to do that, I created and assigned to them material called “Non_def” with Elastic property of Young modulus 200 000 MPa and Poisson ratio of 0,295.

Assembly

All parts were put into assembly. There was no need for any other adjustment of parts.

Step

In this simulation I created 4 “visco” steps:

- Mounting
- Pressure_normal
- Overpressure_7bar
- Overpressure_9bar

As a first step I created “visco” step named “mounting” which represents mounting of membrane plate on flutter membrane. From initial not compressed state (shown on Figure 28) is flutter membrane deformed (compressed) by displacement of membrane plate in vertical direction. This deformation of flutter membrane seals the oscillating chamber of the housing.

Properties of “mounting” step

- Time period = 60 s
- Nlgeom = ON

- Increment size [s] = 1 initial; 1E-05 minimum; 10 maximum
- Creep/swelling/viscoelastic strain error tolerance = 0,02

Rest of the settings remain set as default.

This mounting step is followed by already mentioned pressure loads (regular + over pressures) which are applied on faces that are during real operation in contact with AdBlue. Setting properties of these steps are listed in following Table 6.

Name of step	Regular_pressure	Overpressure_7bar	Overpressure_9bar
Time period [s]	0.12	0.01	0.01
Nlgeom	ON	ON	ON
Increment size [s] initial; min; max	0.0005; 1E-08; 0.01	0.001; 1E-08; 0,001	0.001; 1E-09; 0.001
Creep/swelling/viscoelastic strain error tolerance	0.02	0.02	0.02

Table 6: Properties of each step

Interaction

I created Contact with these properties:

- Tangential behaviour
 - Friction formulation = penalty
 - Friction coef. = 0.1
- Normal behaviour
 - Pressure-overclosure = “Hard” contact
 - Constraint enforcement method = Penalty (standard)
 - Allow separation after contact = YES

I used this Contact property for 2 sets of contact interactions – “housing to flutter membrane” and “flutter membrane to housing”. Properties of this contacts with marked slave and master faces are shown on Figure 29 and Figure 30.



Figure 29: Properties of Housing to Membrane interaction

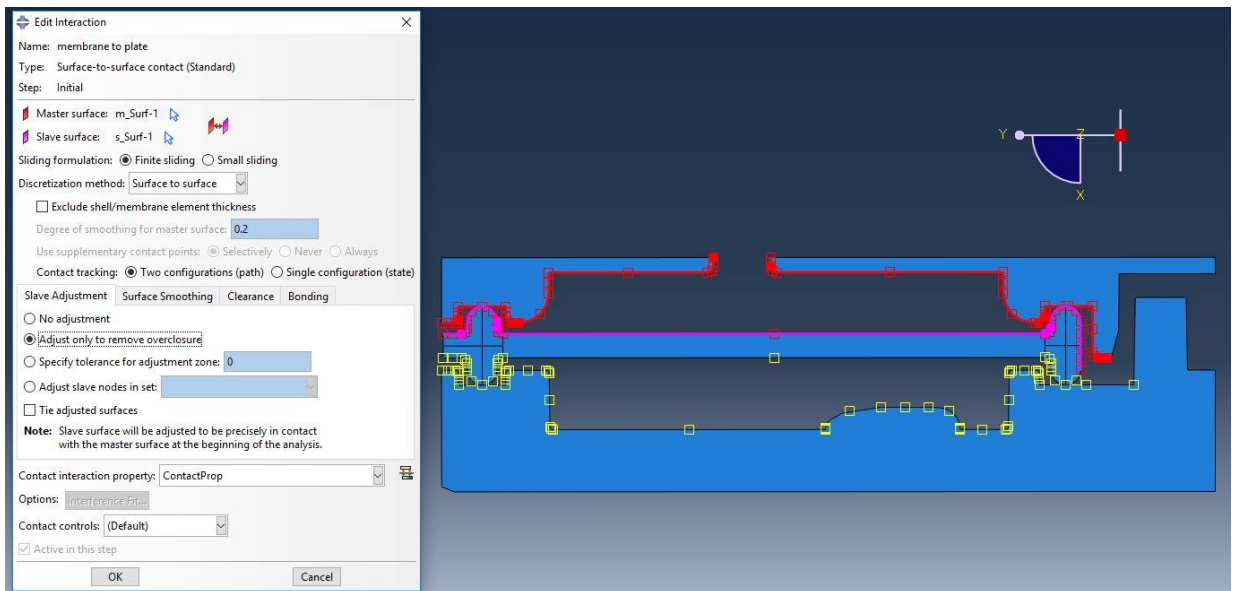


Figure 30: Properties of Plate to Membrane interaction

Load

Boundary conditions

First boundary condition (BC) was named “Housing – fixing”. As it could be guessed from its name, I fixed the housing by using “ENCASTRE” boundary condition on whole part representing the housing. This follows the fact that during real mounting of pressure plate is housing without movement and the plate is pressed down. This BC is propagated through all following steps.

Second BC is called “Plate movement” and via this boundary condition I simulated mounting of the membrane plate. During “Mounting” step I linearly applied 0.8 mm movement of the plate in “X” direction over whole 60 seconds of “mounting step”. I achieved this by using and defining of simple amplitude “Mounting” with tabular values:

Time [s]	Amplitude [mm]
0	0
60	0.8

Table 7: Mounting amplitude

Pressure load

As it was mentioned in “Step” module, for purpose of simulation I created load of pressure type with magnitude of 1 and amplitude of pressure for each step. These amplitudes are used for defining the values of pressure during whole period of each step. Amplitudes for regular pressure and 7/9 bar overpressure are listed in same order in following Table 8, Table 9 and Table 10.

Time [s]	Pressure [Mpa]
0	0
0.01	-0.0551
0.02	-0.01635
0.03	0.009486
0.04	0.005109
0.05	0.001855
0.06	-0.02181
0.07	-0.05838
0.08	-0.0551
0.09	-0.01635
0.1	0.009485
0.11	0.005108
0.12	0

Table 8: Amplitude of regular pressure

Time [s]	Pressure [MPa]
0	0
0.01	0.7

Table 9: Amplitude of 7 bar overpressure

Time [s]	Pressure [MPa]
0	0
0.01	0.9

Table 10: Amplitude of 9 bar overpressure

Mesh

Whole assembly was meshed with CPS4R: A 4-node bilinear plane stress quadrilateral, reduced integration, hourglass control elements. Housing and membrane plate parts were

seeded with global size = 0.4 mm. Edges on these parts with possibility of tight and firm contact with flutter membrane were seeded more fine with approximate element size = 0.2 mm. Flutter membrane was seeded with finest elements of approximate size = 0.1 mm. Final meshed assembly could be seen on following Figure 31.

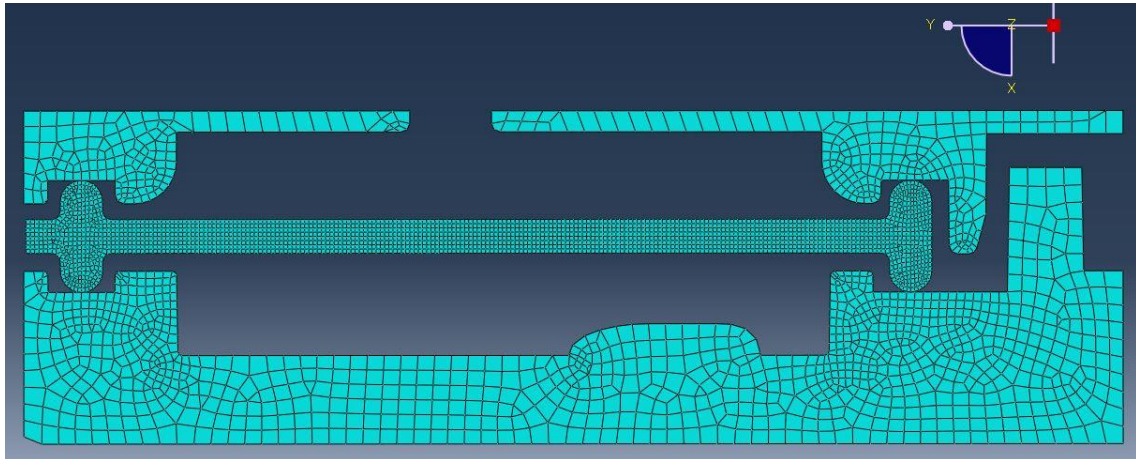


Figure 31: Meshed 2D assembly

Since all settings were done I submit this simulation for solving. After successful completing of simulation, I evaluated the results. Animation of every simulation done in this thesis could be found on attached CD. There will be also enclosed INPUT (.inp) file for all simulations.

8.1 Evaluation of real design results

I focused on locations with the highest stress and strain values during evaluation of each step when pressure load is applied. In normal pressure step was not found any element with exceeding stress and strain (comparing to overpressure steps). If we consider the fact that damage of membrane was for the first time observed in S/S test I decided to focus on overpressure steps, which describe unique and significant phenomena of S/S cycle. For each overpressure step I located the most loaded element and plotted the stress load versus time. Figures will be showing only places with the highest stress, because available space on each page is limited and I wanted to maintain the clearness and readability. On following Figure 32, Figure 33 and Figure 34 is shown the model in start and end of over pressure steps.

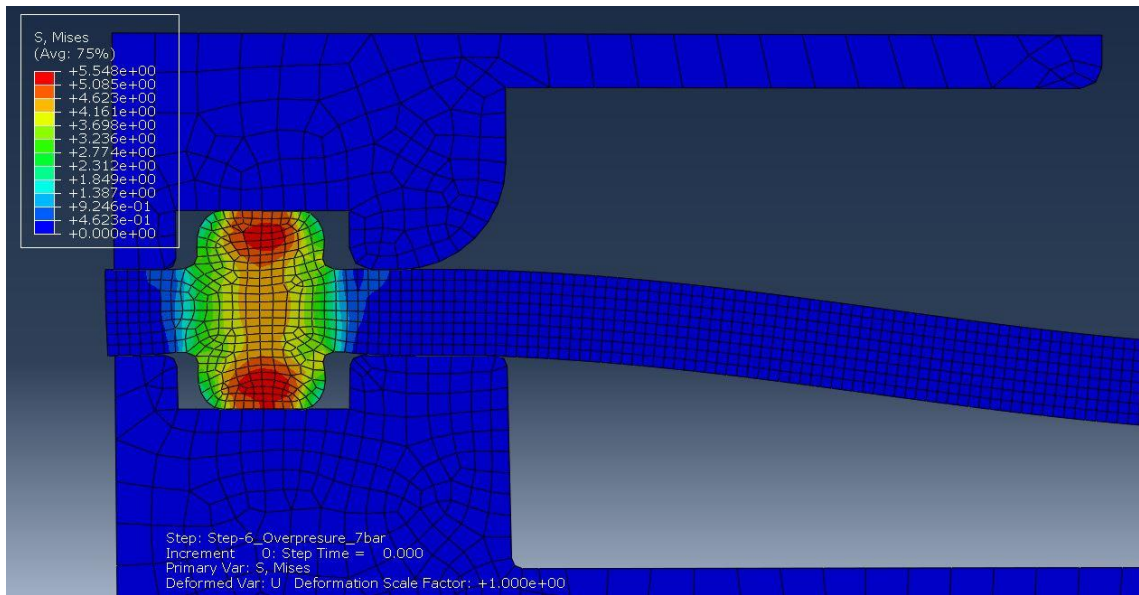


Figure 32: Membrane after compression - end of "Mounting" step

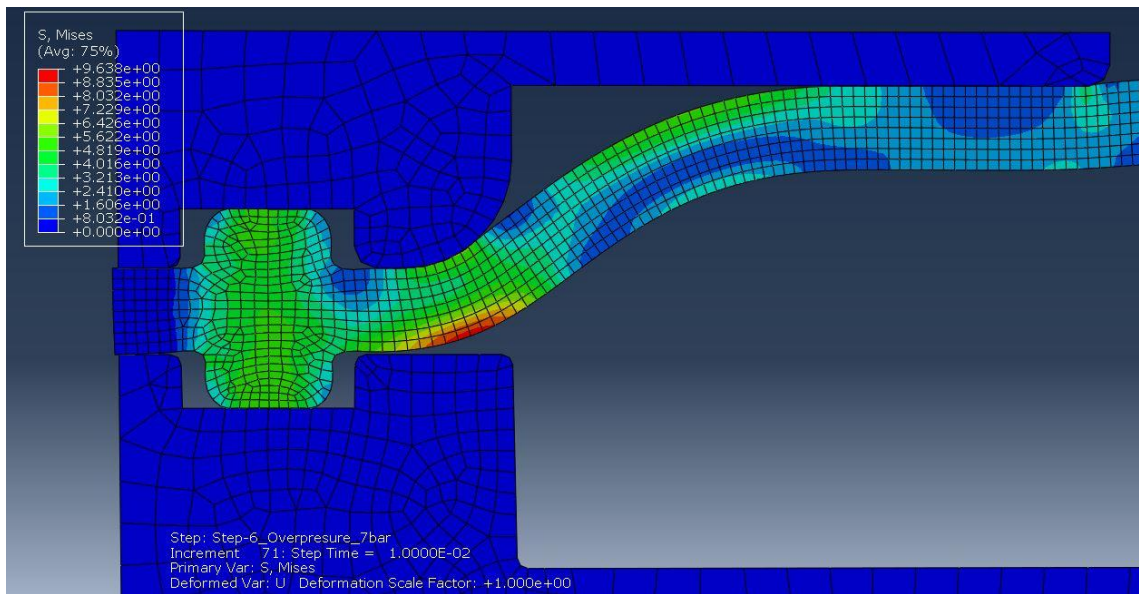


Figure 33: Membrane under overpressure load of 7 bar

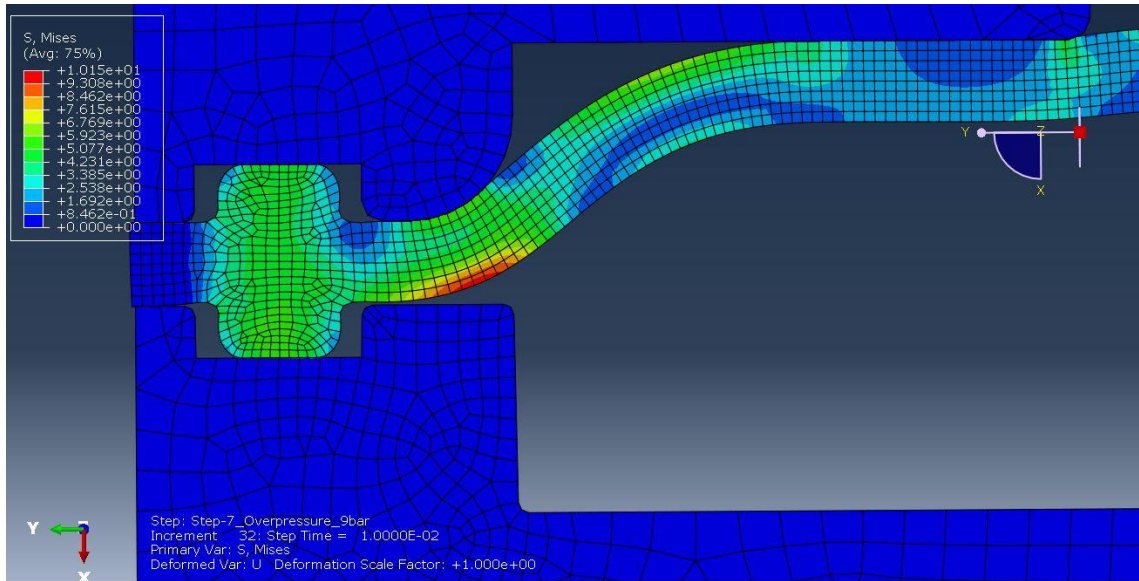


Figure 34: Membrane under overpressure load of 9 bar

As you can see, the most stressed area of flutter membrane is located on the same spot where actual damage was observed. I found the most stressed element and plotted its stress versus time. See Figure 35.

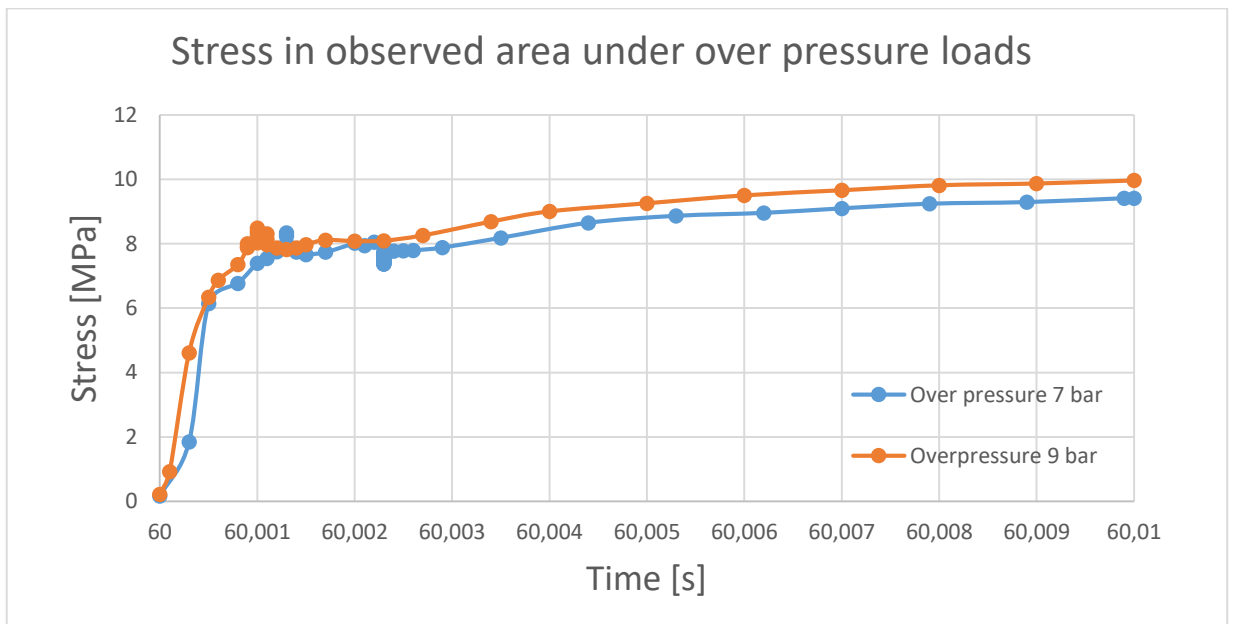


Figure 35: Stress in observed area under over pressusre loads

Disturbances which occur in time interval around time step 60.001 and 60.0025 are caused by settling of flutter membrane in its position (small sliding of fixing rims and their deformation). At the end of the step we achieve stress of 9,46 MPa (7 bar) and 9,69 MPa (9 bar). Difference in stress between 7 bar and 9 bar overpressure is not prominent so for further simulations will be examined only 9 bar overpressure. This stress is generated by fast dynamic loading and stress at break of this material is about 20 MPa, so we are now at 50% of its maximum allowed stress. I tried to obtain fatigue data (S – N curve) for HNBR material, however this data was not available. With respect to these facts I consider these values too high. In order to reduce maximum stress and to support the flutter membrane, I tried to adjust the shape of upper membrane plate. I designed 3 designs with different shape and after that I loaded them in the same way as the actual shape was loaded. Considering the fact that all settings remain same and the only change is in shape of membrane plate, I will not list all settings again. Modifications of design and evaluation of their impact on maximum stress generation will be shown in the following chapter.

8.2 Analysis of modified design results

I designed 3 models with different shapes of membrane plate. You can see these designs on Figure 36, Figure 37 and Figure 38.

I run the simulations with new designs, located the most stressed element and plotted for this elements their stress values over the whole 9 bar over pressure step. After that I compared the results with real, actual design. Figure 36, Figure 37 and Figure 38 show the final deformations for each design modification.

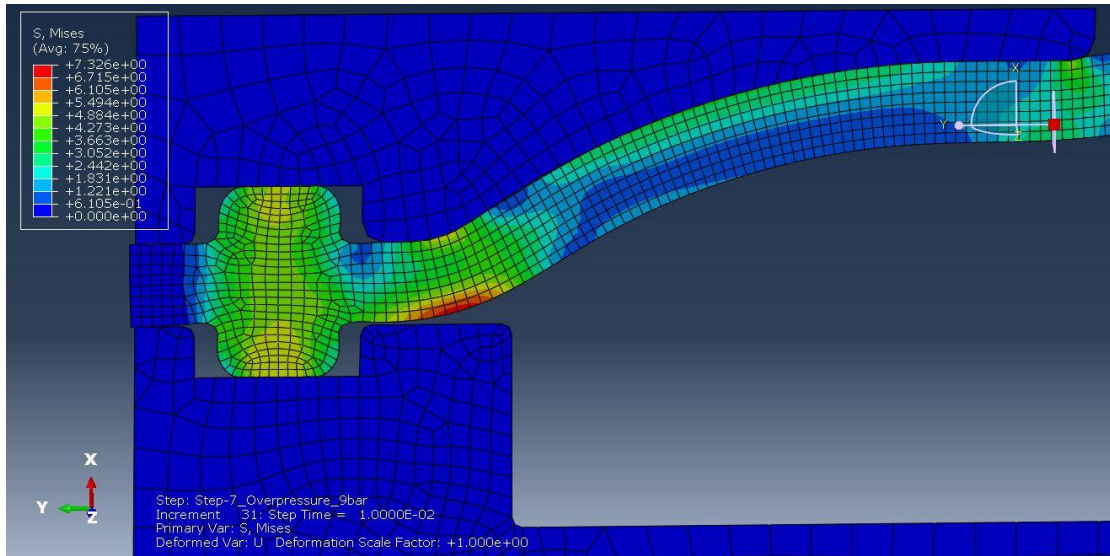


Figure 36: Design optimization 1 - end of 9bar over pressure step

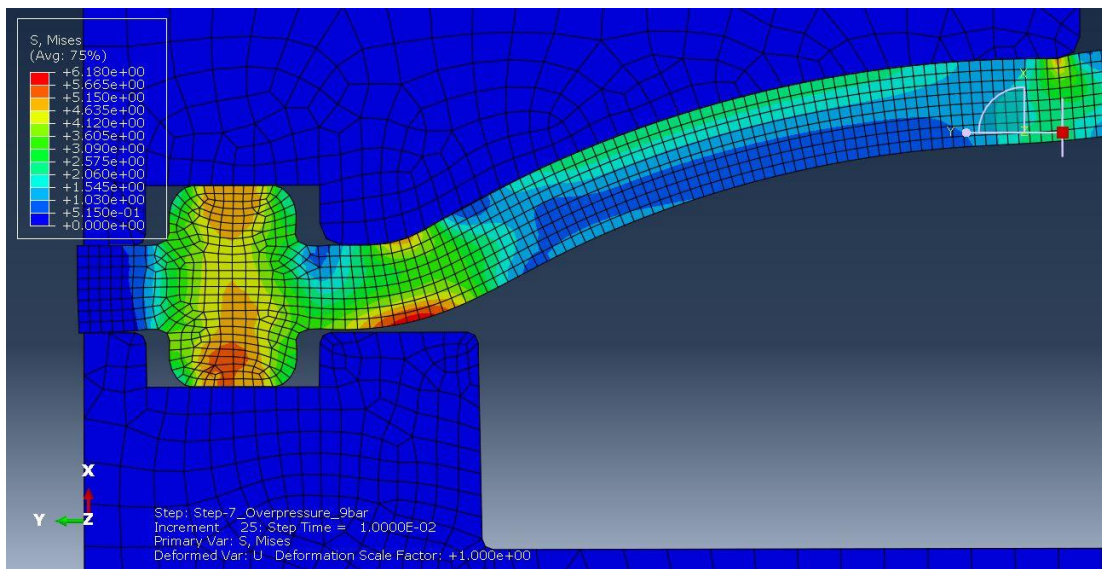


Figure 37: Design optimization 2 - end of 9bar over pressure step

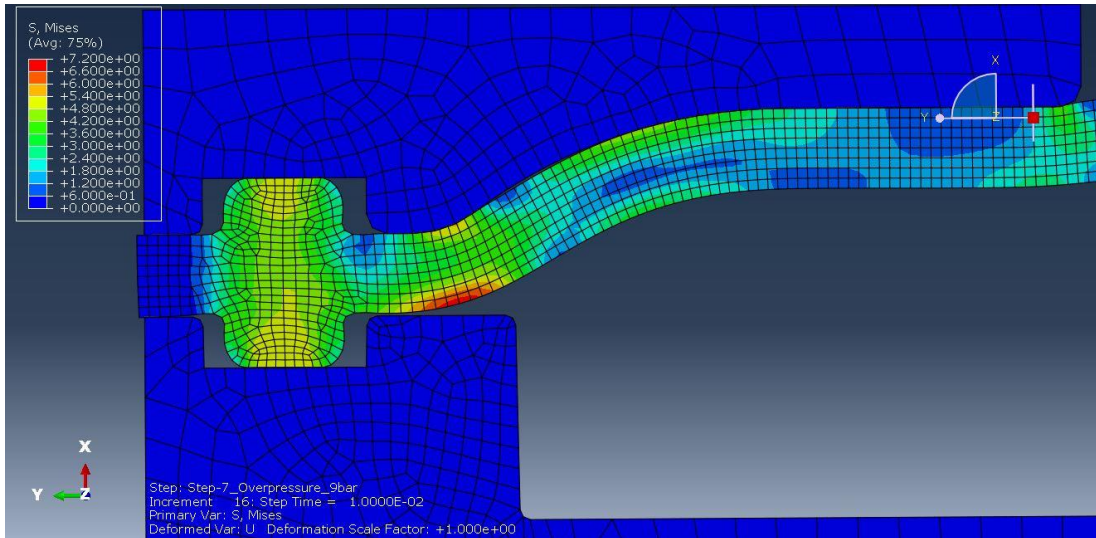


Figure 38: Design optimization 3 - end of 9bar over pressure step

8.3 Comparison of results

You can see the results on following Figure 39. Values of maximal pressure and pressure at the end of step are shown in Table 11.

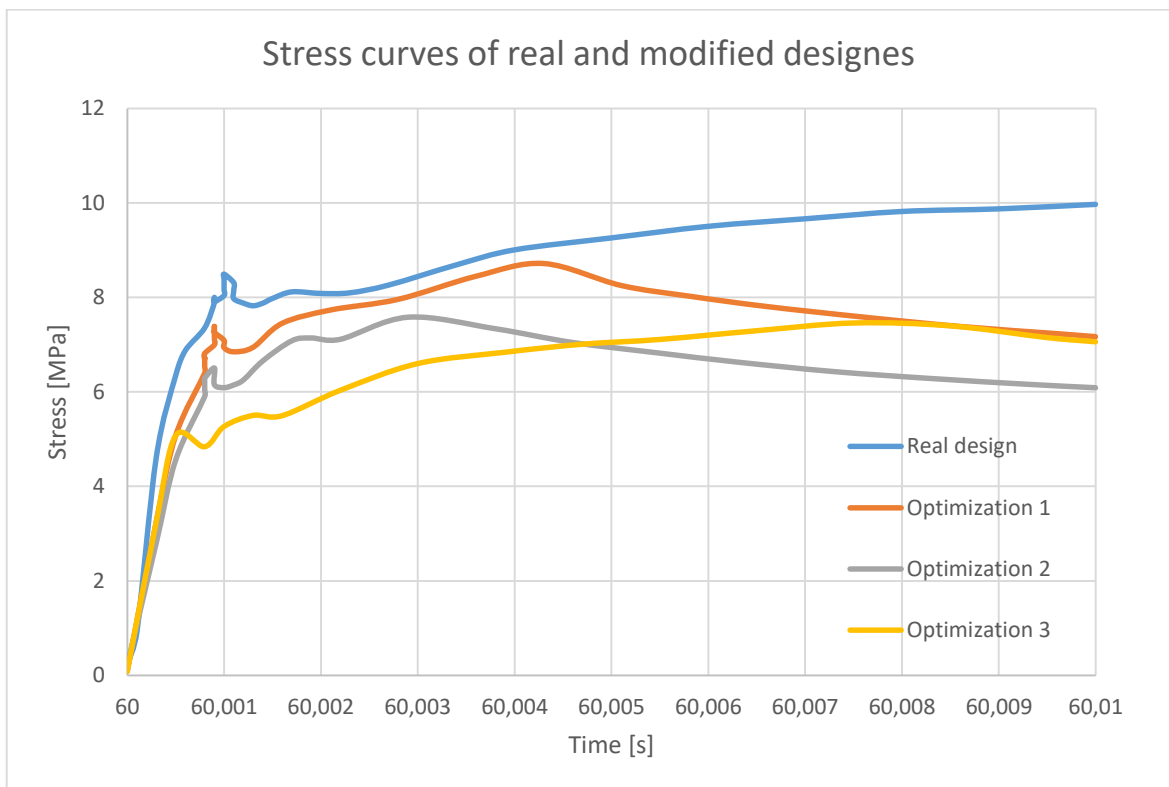


Figure 39: Comparison of modified designs with real design in terms of stress observed in critical area.

	Maximal stress [MPa]	Final stress [MPa]
Real design	9.97	9.97
Optimization 1	8.72	7.17
Optimization 2	7.58	6.09
Optimization 3	7.46	7.06

Table 11: Table of maximal and final stress values of real and modified designs.

If we compare the stress values of optimized designs with real design values, we could observe a percentage improvement in all optimized designs. This improvement is shown as percentage of stress reduction we achieved with modified designs and this enhancement is shown in Table 12.

	Maximal stress reduction [%]	Final stress reduction [%]
Optimization 1	12.5	28.0
Optimization 2	23.9	38.9
Optimization 3	25.18	29.1

Table 12: Improvement achieved by design modifications in terms of percentage improvement comparing to real design.

From the results we can state that:

- There was achieved improvement in all optimization designs.
- Maximal stress was reduced the most in design no. 3.
- Final stressed was reduced the most in design no. 2.
- 3rd design's stress curve has the most convenient characteristic with smoothest disturbances during flutter membrane settling.
- The smallest difference between maximum and final stress is observed in 3rd design.
- After evaluation of all data I find 3rd design as the most beneficial compared to the others.

Conclusion

This master thesis briefly introduced the reader to the topic of selective catalytic reduction - concretely BOSCH DENOXTRONIC system. Aim of the thesis was to simulate and analyse the behaviour of DENOx 2.2 flutter membrane under overpressure condition which were observed in S/S test. In first step it was proved by physical measurement that obtained material data cards from BOSCH company were valid and suitable for HNBR material simulations. Later on it was simulated that we can reduce the stress values in critical areas with design modifications. As the best design modification was chosen 3rd design because of its reasonable reduction of generated stress: about -25 % in maximal stress and -29 % in final stress compared to actual design. This modification also provide convenient shape of Stress – Time curve which is similar to the Stress – Time curve observed on real design. I recommend, on basis of results, to modify the design of membrane plate, test this designs in real S/S test and check the functionality of this new shape including observation of flutter membrane behaviour in transparent model. This modification could be beneficial in way of lowering mechanical loading on the membrane in order to be less susceptible to failure.

This modification could enforce the flutter membrane to be able to sustain this sudden overpressure peak, however the best precaution will be, in my opinion, to generally avoid this overpressure peak or at least significantly reduce the value of this peak. I suppose it could be done by implementing new features into pressure and supply lines or by redesigning of 4/2 reverting valve which cause this pressure peak. This could be the way which might be followed in future research.

References

- [1] SONG, Soonho. Emission Control Systems-Oxides of Nitrogen. *Encyclopedia of Automotive Engineering*. Chichester, UK: John Wiley, 2014, , 16. DOI: 10.1002/9781118354179.auto108. ISBN 9781118354179.
- [2] PARKS, James E. Gas After treatment Systems. *Encyclopedia of Automotive Engineering*. Chichester, UK: John Wiley, 2014, , 1. DOI: 10.1002/9781118354179.auto130. ISBN 9781118354179.
- [3] Emission standards. *DieselNet* [online]. [cit. 2016-04-12]. Available at: <https://www.dieselnet.com/standards/eu/ld.php>
- [4] MAJEWSKI, W. Addy. *Selective Catalytic Reduction* [online]. 2012 [cit. 2016-04-12]. Available at: https://www.dieselnet.com/tech/cat_scr.php
- [5] *Diesel Systems: Denoxtronic 2.2 – Urea Dosing System for SCR Systems* [online]. [cit. 2016-04-15]. Available at: http://www.bosch-mobility-solutions.es/media/ubk_europe/db_application/downloads/pdf/antrieb/en_3/ds_cvdenoxtronic22_de_2010.pdf
- [6] *Material safety datasheet: Diesel Exhaust fluid / AdBlue* [online]. [cit. 2016-04-19]. Available at: <http://www.noco.com/documents/Fuels%20PDS/DEF%20MSDS%20for%20USA.pdf>
- [7] *Selective Catalytic Reduction (SCR)* [online]. [cit. 2016-04-12]. Available at: <http://autoconverterrecyclers.com/selective-catalytic-reduction-scr/>
- [8] MAJEWSKI, W. Addy. Diesel Oxidation Catalyst. *DieselNet* [online]. 2005 [cit. 2016-04-12]. Available at: https://www.dieselnet.com/tech/cat_doc.php
- [9] MAJEWSKI, W. Addy. *Urea Dosing and Injection Systems* [online]. 2015 [cit. 2016-04-13]. Available at: https://www.dieselnet.com/tech/cat_scr_mobile_urea_dosing.php

- [10] KEUPER, Andreas, Jia HUANG, Harald BRESSLER a Wolfgang ALBRECHT. *A Clean Solution – Exhaust Gas Treatment* [online]. , 15 [cit. 2016-04-15]. Available at: https://dc-america.resource.bosch.com/media/us/press_kits_1/conexpo_2014/technical_papers_and_success_stories/rexroth_exhaust_gas_treatment.pdf
- [11] GABLE, Scott a Christine GABLE. Selective Catalytic Reduction and Clean Diesels: Managing Diesel NOx Emissions. *About Autos* [online]. 2016 [cit. 2016-04-15]. Available at: <http://alternativefuels.about.com/od/researchdevelopment/a/scr.htm>
- [12] Size of the vehicle fleet. European environment agency [online]. 2011 [cit. 2016-10-25]. Available at: <http://www.eea.europa.eu/data-and-maps/indicators/size-of-the-vehicle-fleet/size-of-the-vehicle-fleet-2>
- [13] Motorisation rate, by NUTS 2 regions, 2014. *EUROSTAT* [online]. 2016 [cit. 2016-10-25]. Available at: [http://ec.europa.eu/eurostat/statistics-explained/index.php/File:Motorisation_rate,_by_NUTS_2_regions,_2014_\(%C2%B9\)_\(_number_of_passenger_cars_per_1_000_inhabitants\)_RYB2016.png](http://ec.europa.eu/eurostat/statistics-explained/index.php/File:Motorisation_rate,_by_NUTS_2_regions,_2014_(%C2%B9)_(_number_of_passenger_cars_per_1_000_inhabitants)_RYB2016.png)
- [14] Population, EU-28, 1960–2016. *EUROSTAT* [online]. 2016 [cit. 2016-10-25]. Available at: [http://ec.europa.eu/eurostat/statistics-explained/index.php/File:Population,_EU-28,_1960%E2%80%932016_\(%C2%B9\)_\(_at_1_January,_million_persons\)_YB16.png](http://ec.europa.eu/eurostat/statistics-explained/index.php/File:Population,_EU-28,_1960%E2%80%932016_(%C2%B9)_(_at_1_January,_million_persons)_YB16.png)
- [15] *HYDROGENATED NITRILE BUTADIENE RUBBER (HNBR)* [online]. International Institute of synthetic rubber producers, 2012 [cit. 2016-11-6]. Available at: <http://iisrp.com/WebPolymers/AboutRubber/03HNBR16Aug2012.pdf>
- [16] Bosch internal documents